ESTIMATION OF REFERENCE EVAPOTRANSPIRATION IN SELECTED AREAS IN NIGER STATE, NIGERIA

BY

SHEHU, Umar Sanda
MEng/SEET/2017/7614

DEPARTMENT OF AGRICULTURAL & BIORESOURCES ENGINEERING,
FEDERAL UNIVERSITY OF TECHNOLOGY,
MINNA, NIGER STATE, NIGERIA

JANUARY, 2022

ESTIMATION OF REFERENCE EVAPOTRANSPIRATION IN SELECTED AREAS IN NIGER STATE, NIGERIA

BY

SHEHU, Umar Sanda
MEng/SEET/2017/7614

A THESIS SUBMITTED TO THE POSTGRADUATE SCHOOL, FEDERAL UNIVERSITY OF TECHNOLOGY, MINNA, NIGERIA IN PARTIAL FULFILMENT OF THE REQUIREMENTS FOR THE AWARD OF THE DEGREE OF MASTER OF ENGINEERING (MEng) IN AGRICULTURAL & BIORESOURCES ENGINEERING (SOIL AND WATER)

JANUARY, 2022

ABSTRACT

There is need for adequate information on reference evapotranspiration (RET) due to its importance on irrigated agriculture and water resources management. In view of this, the study determined reference evapotranspiration and its trends in Niger State, Nigeria. The meteorological parameters used were derived from National Aeronautics and Space Administration (NASA) and Environmentally Responsible Aviation (ERA) between 1982 and 2020. Daily climatic data and other parameters obtained were available on a 0.5° x 0.5° latitude and longitude global grid. Penman-Monteith formula was used to determine reference evapotranspiration. The trend of reference evapotranspiration was computed using Mann-Kendall. Minna, Shiroro and Bida has maximum RET values of 7.49, 9.22 and 6.03 in 2000 (February) with minimum values of 1.4, 1.36 and 1.57 in 1994 (August), respectively. The results obtained show a statistically significant increasing RET trend in Minna, Shiroro and Bida. In Minna April, July, and September also have the same trend as January in Shiroro which indicated the same level of significant, though have different values. RET trends in May, June, July, and August are similar to January and February in Bida. The implication is that the water required for the crop in September (Minna), April, July, September (Shiroro) and May, June and August (Bida) were the same as February and January. The aerodynamic and net radiation changes the trend of RET in Minna, Shiroro and Bida. The study concluded that Shiroro had the highest maximum RET followed by Minna and Bida in February, 2000.

TABLE OF CONTENTS

LIST OF TABLES

LIST OF FIGURES

LIST OF APPENDICES

CHAPTER ONE

1.0 INTRODUCTION

1.1 Background to the Study

Nearly all of the water utilised in agriculture escapes through evaporation from the soil and through plant transpiration (Kuti *et al*., 2016). Reference Evapotranspiration (RET) is used for water resources management, irrigation management and is influenced by weather conditions and has been modelled as empirically- and physically-based equations (Biggs *et al*., 2016; Huizhi & Jianwu, 2012; Tabari, 2010; Yoder *et al*., 2005; Didari & Ahmadi, 2019 and Allen *et al*., 1998). Evapotranspiration (ET) is an essential part of the water cycle that affects water resources, especially agricultural production (Wang *et al*., 2012). RET is useful in water management, irrigation practices, and surface and subsurface flow. For national hydrological modelling and river basin planning with increased water efficiency (Wang *et al*., 2012), and is essential to understand RET's dynamic response to global warming.

Depending on the input weather variables, RET models are classified as temperature-based, radiation-based, and combination-based models (Senatore *et al*., 2020; Arellano *et al*., 2016; Tabari *et al*., 2013; Itenfisu *et al*., 2003). According to Ma *et al*. (2017), climatic change has been identified not only in individual parameters such as temperature and precipitation but also in RET and is one of the vital components of the hydrological cycle and controls the energy and mass exchange between terrestrial ecosystems and the atmosphere.

RET is influenced by temperature, solar radiation and crop factors, environmental conditions and water resource management. Evapotranspiration (ET) is considered the most significant indicator for climate change and the water cycle (Wang *et al*.,

2014). Most studies have used the FAO Penman-Monteith model (FAO PM56) to estimate RET (Didari & Ahmadi, 2019; Arellano & Irmak, 2016; Pereira *et al*., 2015; Allen *et al*. 1998, 2006; Sabziparvar & Tabari, 2010; DehghaniSanij *et al*., 2004). However, comprehensive analysis of trends for RET is comparatively scarce in Minna, Shiroro and Bida in Niger State, Nigeria.

Numerous studies used empirical equations with metrological data to determine reference evapotranspiration (Gotardo *et al*., 2016). Other methods include energy balance, soil water balance and lysimeter method (Ahmadi & Javanbakht, 2020; Nova *et al*., 2007). The metrological variables that change RET trends are wind speed and relative humidity (Wang *et al*., 2012). Wang *et al*. (2012) showed that wind speed, sunshine hour and net radiation decreases RET in Northern China. Depending on climatic conditions and regions, ET trends may be either increasing or decreasing (Rim, 2009). Some studies have shown a decrease in the evapotranspiration trend over the past decades in many places of the world, however, some has reported the opposite phenomenon that is increasing in evapotranspiration trend (Gao *et al*., 2007; Darshana *et al*., 2013; Irmak *et al*., 2012; Tabari *et al*., 2011; Kousari *et al*., 2013; Hosseinzadeh *et al*., 2014). A number of studies as indicated that the evapotranspiration trend is not determined only by temperature as other parameter could play significant role in the trend of RET. (Mansour *et al*. (2017), (Xu *et al*., (2006); Ohmura and Wild, 2002). Therefore, it is important to determine RET trends in North Central Nigeria, particularly in Minna, Shiroro and Bida where rivers and dams are situated for agricultural activities in a wet and dry season. Evaluating the RET and its trend will aid hydrodynamic modelling, forecasting, and irrigation planning such as scheduling and interval (Shuyun *et al*., 2020).

1.2 Statement of the Research Problem

This study is informed by the following:

(i) Existing works have shown that RET varies with location and no research work has established the variation in RET for Minna, Shiroro and Bida which are different hydrological response units in Niger State.

(ii) Increase in RET has been associated with temperature and studies has shown increasing trend temperature for Minna, Bida and Shiroro.

1.3 Justification of the Study

Water cycle and agricultural water management are dependent on reference evapotranspiration, which means that accurate reference evapotranspiration forecasts are critical to understanding the hydrological cycle and managing irrigation. Understanding the evapotranspiration complexity of agricultural land will allow for optimum crop water requirements to be determined in dry and rainy seasons, allowing for prediction of irrigation management (Kuti *et al*., 2016). Estimation of reference evapotranspiration and its trend will enable the water engineer and agriculturist in Minna, Shiroro and Bida to know the factor influencing either increasing or decreasing in trend of reference evapotranspiration.

1.4 Aim and Objectives of the Study

The study aims to estimate reference evapotranspiration in Minna, Shiroro and Bida. The specific objectives are to:

i. determine reference evapotranspiration
ii. determine the trend in reference evapotranspiration (RET) in each location, and
iii. assess the major factor influencing the reference evapotranspiration in the Study Area.

1.5 Scope of the Study

The research covers the determination of RET in Minna, Shiroro and Bida, trend analysis of RET trend and assessing the factors causing the trend of RET in selected locations.

1.6 Limitation of the Study

The study is fundamentally limited in terms of design due to: (a) time limits for detail estimation of reference evapotranspiration on Minna, Shiroro and Bida basins and (b) an insufficient amount of data in the study area.

CHAPTER TWO

2.0 LITERATURE REVIEW

2.1 The Hydrologic Cycle

Hydrology is the study of the distribution, circulation, and physical properties of water throughout the Earth and its atmosphere, over a range of time and space (Hickman, 2011). The hydrologic cycle and its complex series of phase changes and interconnected flow is schematically represented as seen in Figure 2.1.

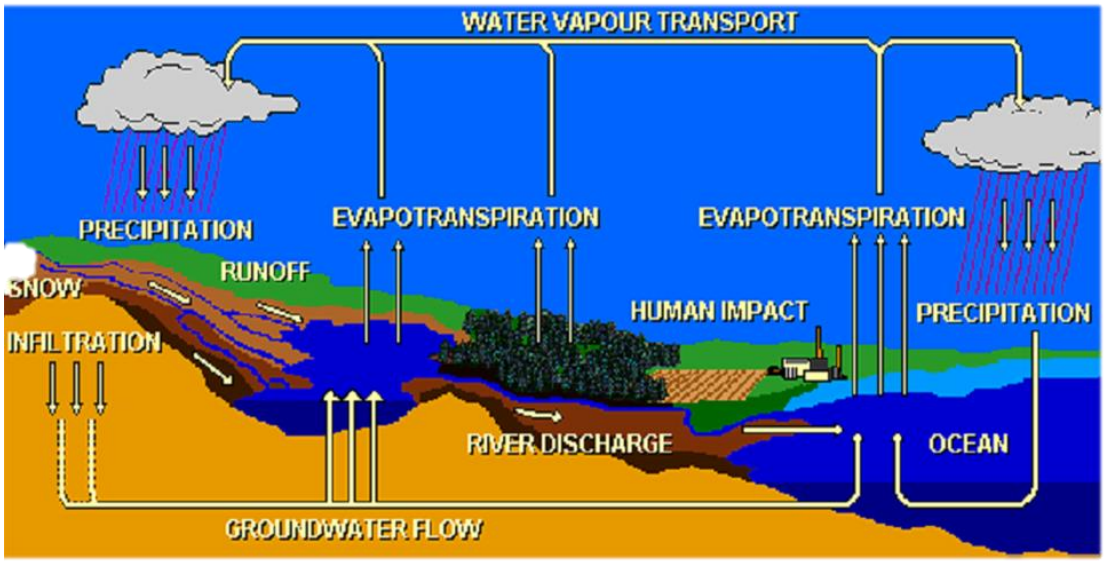

Figure 2.1: Hydrological cycle

The circle has neither a beginning nor an end, but the concept of the hydrologic cycle commonly begins with the water of the oceans, since it covers about three fourths of the earth's surface. Radiation from the sun evaporates water from the oceans into the atmosphere (Richard & Steven, 2007). The water vapour arises and collects to form clouds. Under certain conditions, the cloud moisture condenses and falls back to the earth as rain, hail, sleet, or snow. Precipitation reaching earth surface may be intercepted by vegetative materials, infiltrate into the ground, and flow over the land surface as runoff or evaporated water. Evaporation may be from the surface of the ground, from free water

surface or from leaves of plants through transpiration. Some of the precipitation after wetting the foliage and ground surface move over land to streams as runoff while the other part infiltrate the soil (Richard & Steven, 2007). Much of the water that enters the soil is detained in the plant root zone and eventually drawn back to the surface by plant or by soil capillarity. Some of it however, soaks below the plant root zone and under the influences of gravity continues to move downward until it enters the ground water reservoir (Richard & Steven, 2007). On joining the body of ground water, the percolating water may move through the pores of saturated subsurface materials and may reappear at the surface in areas at lower elevations as subsurface flow. The streams carrying both surface runoff and subsurface flow eventually flow back to the oceans to restart the cycle (Richard & Steven, 2007).

2.1.1 Radiation

The solar radiation received at the top of the earth atmosphere on a horizontal surface is known as the extra-terrestrial radiation (Ra). The values of extra-terrestrial radiation depend on season change, the position of the sun, and of course the length of the day. It therefore stands that the extra-terrestrial radiation is a function of latitude, and the date and time of the day. The solar constant is the radiation striking a surface perpendicular to the sun's ray at the top of the earth's atmosphere and it is some 0.082 $MJm^{-2}min^{-1}$. If the position of the sun is directly overhead, the incidence angle of extra-terrestrial radiation is zero. In this case, extra-terrestrial radiation is some 0.082 $MJm^{-2}min^{-1}$ (Kosa, 2003). The amount of radiation penetrating from the atmosphere to a horizontal plane is known as solar or shortwave radiation (Rs). The sun emits energy by electromagnetic waves that include short wavelengths, so solar radiation is referred to as shortwave radiation. In this atmosphere, radiation is absorbed, scattered, or reflected by gases, clouds, and dust. For

cloudless day, the solar radiation is about 75 % of the extra-terrestrial radiation, while it is about 25 % of the extra-terrestrial radiation on a cloudy day (Kosa, 2003).

The solar radiation which is also known as global radiation is a summation of direct shortwave radiation from the sun and diffuse sky radiation from all upward angles. Relative shortwave radiation (Rs/Rso) is a relationship between shortwave radiation (Rs) and clearly-sky solar radiation (Rso). The shortwave radiation is solar radiation that actually reaches the earth's surface in a given time, while clearly-sky solar radiation is solar radiation that reaches to the same area with a clearly-sky condition. The relative shortwave radiation is affected by the cloudiness of atmosphere. On a cloudy day, the ratio is smaller than on a cloudless day. The range of this ratio is between 0.33 (cloudy condition) to 1.00 (cloudless condition) (Kosa, 2003). The cloudiness in the atmosphere is revealed by the relative sunshine duration, (n/N). It is the relationship between the actual duration of sunshine (n) and the maximum possible duration of sunshine, or daylight hours (N). For the cloudless condition, n is equal to N, while n and n/N are nearly zero for the cloudy condition. The maximum possible duration of sunshine, or daylight hours (N), depends on the position of the sun, so it is a function of latitude and date. The daily values of N throughout a year differ with latitude. The relationship between reflected radiation and total incoming radiation is known as Albedo (α), it varies with both characteristics of the earth's surface and the angle of incidence, or the slope of ground surface. Albedo can be more than 0.95 for freshly fallen snow, and it is smaller than 0.05 for wet bare soil. The range of Albedo for green vegetation is about 0.20-0.25 and Albedo for the green grass reference is 0.23. Net solar radiation (Rns) is the fraction of the solar radiation that is reflected from the ground surface. It can be expressed by the equation 2.1:

$$R_{ns} = (1-\propto)R_s \quad (2.1)$$

where,

Rns is net solar radiation, $\propto$ is Albedo, Rs is solar radiation (short wave radiation).

The difference in value between outgoing and incoming longwave radiation is known as net longwave radiation (RnL). It is solar radiation absorbed by the earth and turned to heat energy. Since the temperature of the earth is less than the sun, so the earth emits longer wavelengths (Kosa, 2011). Terrestrial radiation is referred to as longwave radiation. The emitted longwave radiation (RI, up) is absorbed by the atmosphere or lost into space. The longwave radiation received by the atmosphere (RI down) increases its temperature (de Noblet-Ducoudré, & Pitman, 2021). Therefore, the earth's surface both emits and receives longwave radiation. The value of outgoing longwave radiation is normally more than the incoming longwave radiation, so the net longwave radiation is used to present the energy loss. Net radiation (Rn) is the difference in value between incoming and outgoing radiation of both short and long wave lengths. It is the balance among energy absorbed, reflected, and emitted by the earth's surface. The net radiation is also the difference in value between the incoming net shortwave (Rns) and the net outgoing longwave (RnI) radiation. It is a positive value during daytime, while it is negative value during nighttime (Jia *et al.*, 2018). For the total daily value, it is a positive value except for the condition of high latitude. Soil heat flux (G) is energy that is used in heating the soil. It is a positive value under the condition of warming soil and negative under cooling soil (Kosa, 2003).

2.1.2 Rainfall

Precipitation is a part of the science of meteorology which has to do with the atmospheric phenomena of heat, moisture and air movement. It may occur in any of a number of forms

and may change from one form to another during its descent. The forms of precipitation consisting of fallen water droplets may be classified as drizzle or rain. Drizzle itself consists of quite uniform precipitation with drops less than 0.5mm on diameter, while rain consists generally of larger particles. It is on record also that precipitation may also occur as frozen water particles including snow, sleet, and hail. Characteristically, each of these has its formative procedure; snow is composed of a grouping of small ice crystals known as snowflakes. Sleet forms when raindrops are falling through air having a temperature below freezing. A hail stone is an accumulation of many thin layers of ice over a snow pellet. Moisture is also made available by direct condensation and absorption from the atmosphere as dew (Schwab *et al.,* 1981). Condensation is the formation of water droplets in the clouds. Moisture is always present in the atmosphere, even in a cloudless day. For precipitation to occur, some mechanism is required to cool the air sufficiently to bring to or near saturation. The large-scale cooling needed for significant amount of precipitation is achieved by lifting the air. This is accomplished by convective systems resulting from unequal radiative heating or cooling of the earth surface and atmosphere or by convergence caused by orographic barriers (Linsley *et al.,* 1982).

The presence of condensation nuclei is always needed for the formation of raindrops to take place, it is upon this that the droplets crystal form. These nuclei are small particles of various substances, usually ranging in size from about 0.1 to 10μm in diameter. These particles are called aerosols. During the initial occurrence of condensation, the droplets or ice particles are very small and are kept aloft by motion of the air molecules. Once droplets are formed they also act as condensation nuclei. These droplets tend to repel one another, but in the presence of an electric field in the atmosphere they attract one another and are heavy enough to fall through the atmosphere. Some of the droplets evaporate in the atmosphere, some decrease in size by evaporation and some increase in size by impact

and aggregation. A variety of instruments and techniques have been developed for measuring the amount and intensity of precipitation. All forms of precipitation are measured on the basis of the vertical depth of water that would accumulate on a level of surface if the precipitation remained where it fell. In the metric system precipitation is measured in millimeters and tenths (Linsley *et al.*, 1982). Rainfall/precipitation measurement is very important with regards to the estimation of evapotranspiration.

2.1.3 Infiltration

Infiltration is the process by which water on the soil surface enters the soil. Some precipitation lost due to infiltration may return to streams or interflow and may contribute to runoff. Infiltration is the main source of soil water to sustain the growth of vegetation and deep percolation, recharge of ground water supply of wells, springs and streams. The rate decreases as the soil becomes saturated, and it is affected by soil characteristics including ease of entry, storage capacity, and transmission rate through the soil. The soil texture and structure, and rainfall intensity, all play important role in controlling infiltration rate and capacity. Infiltration rate is a measure of the rate at which the soil is able to absorb rainfall or irrigation water. While infiltration capacity is the maximum rate that water can enter a soil in a given condition. Infiltration is quite important in hydrological studies. It is measured in millimeter per hour. The infiltration rate is used for the computation of the water loss due to infiltration for the purpose of determining surface runoff. The knowledge of the infiltration character of a soil is basic information required for designing efficient irrigation system.

2.1.4 Transpiration

Transpiration consists of the vaporization of liquid water contained in plant tissues and the vapour removal to the atmosphere. Crops predominantly lose their water through

stomata. So transpiration is a process through which water vapour passes into the atmosphere through the tissue plants or stomata. These are small openings on the plants leaf through which gases and water vapour pass. The water, together with some nutrients, is taken up by the roots and transported through the plants. The vaporization occurs within leaf, namely the inter-cellular spaces, and the vapour exchange with the atmosphere is controlled by the stomatal aperture. Transpiration mainly occurs during daylight hours. Transpiration, like direct evaporation, depends on the energy supply, vapour pressure gradient and wind. Hence, radiation, air temperature, air humidity, and wind terms should be considered when assessing transpiration. The soil water content and the ability of the soil to conduct water to the roots also determine the transpiration rate, as do water logging and soil water salinity. The transpiration rate is also influenced by crop characteristics, environmental aspects and cultivation practices. Plant roots can never remove the water completely from the soil. The water contents of the soil when the plant ceases to extract water is called the wilting coefficient. Plants require a large quantity of water for their growth. The rate of transpiration depends upon the growth period of the plant. Transpiration ratio is the ratio of the total weight of water transpired during the entire growth period to the weight of dry matter produced by the plant.

$$transpiration\ ratio = \frac{weight\ of\ water\ transpired}{weight\ of\ dry\ matter\ produced} \quad (2.2)$$

For most crops, the transpiration ratio varies from 300 to 800 (Arora, 2002).

2.1.5 Evaporation

Water can exist in the natural environment in three different forms or states: solid (ice), liquid and gas. The process by which water changes from a liquid to a gas is known as evaporation. Above the water surface are the water molecules in the form of water vapour which are always found above liquid water. From time to time one of the water molecules (vapours) on the surface get knocked away or evaporates as they are always found moving

around. Evaporation occurs when molecules of water obtain high kinetic energy to eject themselves from the water surface into the atmosphere. The amount of energy used by a unit mass of water from the liquid state to the vapour state at constant temperature is known as the latent heat of evaporation, which is above 585 calories per gram. The rate of evaporation is influenced by solar radiation, air temperature, vapour pressure, wind, and minimally by atmospheric pressure (Linsley *et al.,* 1982). Vapour molecules continuously leave the water during evaporation.

The motion of these molecules produces a pressure on the water surface, which is known as vapour pressure. Therefore, vapour pressure is due to vapour molecules present in air. If there is continuous supply of heat energy, more and more molecules accumulate and finally a state is reached when the air above the free surface becomes saturated with vapours and it cannot accommodate more vapours. The partial pressure exerted by the water vapours at this stage is called the saturation vapour pressure(s). The saturation pressure increases with an increase in temperature if the vapour pressure in the air above the water surface remains less than that of the water surface, evaporation continues. As soon as the vapour pressure reaches the saturation pressure, evaporation stops. Many evaporation formula for free water surface as based upon Dalton's law. Dalton's law states that rate of evaporation depends on the difference between the saturation vapour pressure and the vapour pressure in the air above. It is given as:

$$E_a = C[e_s - e_a] \qquad (2.3)$$

Where:

e_s is the saturated vapour pressure at the temperature of the water surface in mm of Hg,

e_a is the actual vapour pressure of the air,

C is a constant that depends on barometric pressure, wind velocity and E_a is the rate of evaporation [cm/day].

For evaporation to continue, the following three conditions must be satisfied:

i. a constant supply of water,

ii. constant supply of heat, and

iii. a vapour deficit.

Evaporation shall continue till $e_s = e_a$. On the other hand, if ea is greater than es, condensation will take place. In that case, more molecules return to the water surface than those that leave it (Arora, 2002). Evaporation measurements from free water surface are commonly made using evaporation tanks or pans.

2.1.6 Evapotranspiration

By definition Evapotranspiration (ET) is the loss of water from a vegetated surface through the combined processes of evaporation and plant transpiration. The term evapotranspiration comes from combing the prefix 'evapo' (for soil evaporation) with the word transpiration. Both soil evaporation and plant transpiration represent evaporative processes. The difference between the two rests in the path by which water moves from the soil to the atmosphere. Water lost by transpiration must enter the plants via the roots, and then pass to the foliage where it is vaporized and lost to the atmosphere through tiny pores in the leaves known as stomata; while water lost through soil evaporation passes directly from the soil to the atmosphere. Evaporation is governed by the availability of water in the top soil and the fraction of solar radiations reaching soil surface. The amount of solar radiation reaching soil surface varies with the degree of crop shading. While transpiration itself is a function of crop canopy and soil water status. Evaporation has been found to dominate the ET by as much as 100 % during early stages of crop growth, while transpiration contributes to nearly 90 % of the ET for a fully matured crop (Allen

et al., 1998). Evapotranspiration (ET) is classified into either reference evapotranspiration (RET) or crop evapotranspiration (ETc).

Evapotranspiration (ET) data are usually presented as a depth of water loss over a particular period of time in a manner similar to that of precipitation. Common unit for ET are millimeters/day. However in others, the time could be an hour, month, decade or even an entire growing period or year in units of water depth.

2.1.7 Reference evapotranspiration

The evapotranspiration rate from a reference surface, not short of water is called reference crop evapotranspiration and is denoted as RET. The reference surface is a hypothetical grass reference crop with specific characteristics. The concept of the reference evapotranspiration was introduced to study the evaporative demand of the atmosphere independently of crop type, crop development and management practices. Relating ET to a specific surface provides a reference to which ET from other surfaces can be related. In other words, RET determines the loss of water from a standardized vegetated surface which helps in fixing the base value of ET specific to that site. The only factors affecting RET are climatic parameters (Gedamu, 2017; Barella-Ortiz *et al.,* 2013).

Consequently, RET is a climatic parameter and can be computed from weather data. RET expresses the evaporating power of the atmosphere at a specific location and time of the year and does not consider the crop characteristics and soil factors. RET can be estimated from meteorological data using empirical and semi empirical equations. So many empirical methods have been developed to estimate evapotranspiration from different climatic variables. Such methods include Blaney-Criddle method and Penman-Montheith method. Certain factors are quite considered in the selection of method. One of the most important factors governing the selection of a method is the data availability. For

example, Blaney-Criddle only requires the temperature data while the Penman-Monteith requires additional parameters such as wind, speed, humidity, and solar radiation. In addition, since the Blaney-Criddle method is used to calculate monthly method Kc values (crop coefficient) as compared to daily, less data is needed for this method. Several studies have been conducted over the years to evaluate the accuracy of different RET estimation methods. Most of these studies have concluded that Penman-Monteith equation in its different forms provides the best RET estimate under most conditions. Therefore, FAO, the Food and Agricultural Organization recommends FAO - Penman Montheith (FAO-PM) method as the sole standard method for computing RET (Allen *et al.*, 1998). FAO-PM provides accurate RET estimates for weekly or even hourly periods. The FAO-PM is also selected because it closely approximates grass RET at the location evaluated, It is physically based and explicitly incorporates both physiological and aerodynamic parameters.

2.1.8 Crop evapotranspiration

The crops evapotranspiration (ETc) under standard condition is the evapotranspiration from disease-free, well fertilized crops, grown in large fields, under optimum soil water conditions, and achieving full production under the given climatic conditions. That means that actual crop water use depends on climatic factors, crop type, crop growth/development and crop management practices. While RET provides the climatic influence on crop water use, the effect of crop type and management is addressed by ETc Factors affecting ETc such as ground cover, canopy properties and aerodynamic resistance for a crop are different from the factors affecting reference crop; therefore ETc differs from RET. The characteristics that distinguish field crops from the reference crop are integrated into a crop factor or crop coefficient (Kc) (Allen *et al.,* 1998). Crop evapotranspiration can be calculated from climatic data and by integrating directly the

crop resistance, albedo and air resistance factor in the Penman-Montheith approach. The Penman-Montheith method is used for the estimation of the standard reference crop to determine its evapotranspiration rate, RET. Experimentally determined ratio of ETc/RET, is the crop coefficient (Kc) and it is used to relate ETc to RET.

$$ET_c = K_c ET_o \quad (2.4)$$

Due to variation in the crop characteristics throughout its growing season Kc for a given crop changes from sowing till harvest because of variation in crop characteristics.

2.2 Factors Affecting Evapotranspiration

The rate of evapotranspiration for a given environment (vegetation) is a function of certain critical factors. Weather parameters, crops characteristics, management and environmental aspects are factors affecting evaporation and transpiration.

2.2.1 Weather parameters

The principal weather parameters affecting evapotranspiration are radiation, air temperature, humidity and wind speed. Several procedures have been developed to assess the evaporation rate from these parameters. The evaporation power of the atmosphere is expressed by the reference evapotranspiration (RET). The reference evapotranspiration represents the evapotranspiration from a standardized vegetated surface.

2.2.2 Crop factors

The crop type, variety and development should be considered when assessing the evapotranspiration from crops grown in large, well-managed fields. Differences in resistance to transpiration, crop height, crop roughness, reflection, ground cover and crop rooting characteristics result in different ET levels in different types of crops under identical environmental conditions. Crop evapotranspiration standard conditions refers to the evaporating demand from crops that are grown in large fields under optimum soil

water, excellent management and environmental conditions, and achieve full productions under the given climatic conditions (Behera & Bahidar, 2020).

2.2.3 Management and environmental conditions

Factors such as soil salinity, poor land fertility, limited application of fertilizers, the presence of hard or impenetrable soil horizons, the absence of control of diseases and pests and poor soil management may limit the crop development and reduce the evapotranspiration. Other factors to be considered when assessing ET are ground cover, plant density and the soil water content. The effect of soil water content on ET is conditioned primarily by the magnitude of the water deficit and the type of soil. On the other hand, too much water will result in water logging which might damage the root and limit root water uptake by inhibiting respiration. When assessing the ET rate, additional consideration should be given to the range of management practices that act on the climatic and crop factors affecting the ET process. Cultivation practices and the type of irrigation method can alter the micro climate, affect the crop characteristics or affect the wetting of the soil and crop surface. A wind breaker reduces wind velocities and decreases the ET rate of the field directly beyond the barrier (Yang *et al.,* 2013).

The effect can be significant especially in windy, warm and dry conditions, although evapotranspiration from the tree themselves may affect any reduction in the field. Soil evaporation in a young orchard, where trees are widely spaced, can be reduced by using a well-designed drip or trickle irrigation system. The drippers apply water directly to the soil near trees, thereby leaving the major part of the soil surface dry, and limiting the evaporation losses. The use of mulches, especially when the crop is small, is another way of substantially reducing soil evaporation. Anti-transpirants, such as stomata-closing,

filming forming and reflecting materials, reduce the water losses from the crop and hence the transpiration rate (Shirish, 1996).

2.2.4 Crop coefficient

The values of crop-coefficient (Kc), increase as a crop grows, reaches a plateau as crop growth attain peaks, and decreases as the crop reaches maturity. Therefore, crop coefficients are dependent mostly on crop type and stage of growth and not on climate conditions. The idea is that crop coefficient remains essentially the same for the same crop, location and climate, notwithstanding, so once the Kc values for a given crop and variety are determined, they can be applied almost anywhere. If this transferability were not valid it would not make much sense to determine ETc through such a period of time instead, it would be necessary to calibrate ET equations for each site and each crop type individually. So, with crop coefficients it is only necessary to estimate RET at a given site, then multiply by the appropriate value of the Kc to arrive at the estimated evapotranspiration rate of the crop. The crop evapotranspiration differs distinctly from the reference evapotranspiration (RET) as the ground cover, canopy properties and aerodynamic resistance of the crop are different from grass. The effects of characteristics that distinguish field crops from grass are integrated into the Kc. In the crop coefficient approach, crop evapotranspiration is calculated by multiplying RET by Kc. Kc is computed as the ratio of reference and crop ET as presented in equation (2.4).

Numerous studies have been carried out over the years to develop the Kc for different agricultural crops. Since most of the studies have been specific to one or two crops, Dorrenbus & Pruitt (1977) prepared a comprehensive list of Kc for various crops under different climatic conditions by compiling results from different studies. Similar list of Kc was also given by Allen *et al.* (1998) and Doorenbus & Kassam (1979). However, Kc

for a crop may vary from one place to another depending on factors such as climate, soil, crop type, crop variety, irrigation methods (Kang *et al.,* 2003). Thus, for accurate estimation of the crop water use, it is important to use Kc from the same region. Researchers have emphasized the need for regional calibration of Kc under climatic conditions (Dorrenbus & Pruitt, 1977; and Kang *et al.,* 2003). It therefore stands that the reported values of Kc should be used only in situations where regional data are not available.

2.3 ET Empirical Equations

2.3.1 Penman-monteith

Crop evapotranspiration can also be derived from meteorological and crop data by means of FAO Penman-Montheith equation as in the equation below:

$$ET_o = \frac{0.408\Delta(R_n G) + \gamma \frac{900}{T+273} U_2 \left(e_{s-e_a}\right)}{\Delta + \gamma(1 + 0.34U_2)} \quad (2.5)$$

Where,

ET_o is reference evapotranspiration [mm day^{-1}],

Rn is net radiation at the crop surface [MJ m^{-2} day^{-1}],

G is soil heat flux density [MJ m^{-2} day^{-1}],

T is mean daily air temperature at 2 m height [°C],

U_2 is wind speed at 2 m height [ms^{-1}],

e_s is saturation vapour pressure [kPa],

e_a is actual vapour pressure [kPa],

e_s-e_a is saturation vapour pressure deficit [kPa],

Δ is slope vapour pressure curve [kPa °C^{-1}],

γ is psychometric constant [kPa °C^{-1}].

2.3.2 Hargreave

Hargreaves-Samani (HS) requires meteorological data that is comparatively scarce (global solar radiation, air humidity and wind speed mainly) limit the use of the PM-FAO method in many locations. Allen *et al*. (1998) recommended applying Hargreaves–Samani expression for situations where only the air temperature is available. The Hargreaves-Samani formulation (HS) is an empirical method that requires empirical coefficients 190 calibrating (Hargreaves & Samani, 1982, 1985). The Hargreaves and Samani (Hargreaves & Samani, 1982, 1985) method is given by the following equation.

$$ET_0 = 0.0135 \cdot K_{RS} \cdot 0.408 \cdot H_0 \cdot (T_m + 17.8) \cdot (T_x - T_n)^{0.5} \quad (2.6)$$

Where RET is the reference evapotranspiration (mm day-1);

Ho is extraterrestrial radiation (MJ·m-2·d-1);

kRS is the Hargreaves empirical coefficient,

Tm, Tx and Tn are the daily mean, maximum and minimum air temperature (°C), respectively.

The value kRS was initially set to 0.17 for arid and semiarid regions 195 (Hargreaves & Samani, 1985). Hargreaves (1994) later recommended to use the value of 0.16 for interior regions and 0.19 for coastal regions. Daily temperature variations can occur due to other factors as topography, vegetation, humidity, among others, thus contemplating a fixed coefficient may lead to errors. In this study, we use the 0.17 as original coefficient (HSo) and the calibrated coefficient kRS (HSc). The kRS reduces the inaccuracy and consequently thus improving the estimation of RET.

2.3.3 Blaney-morin Nigeria

The Blaney-Morin-Nigeria (BMN) model was created to estimate reference evapotranspiration (RET) in Nigeria. The Blaney-Morin-Nigeria (BMN) model is stated in equation 2.7 (Duru, 2016).

$$PET = p\frac{(0.45t+8)(H-R^m)}{100} \quad (2.7)$$

Where PET = potential evapotranspiration (mm/day). t is the mean monthly temperature (°C), R is the mean monthly relative humidity, H and m are model constants of 520 and 1.31, respectively. Duru (2016) optimised reference evapotranspiration in Enugu and the optimised BMN model is shown in equation 2.8.

$$\mathrm{ET_0} = \mathrm{rf}\frac{(0.45\mathrm{T_a}+8)(392-\mathrm{R}^{1.19})}{100} \quad (2.8)$$

2.4 Other ET Methods

2.4.1 Energy balance method

Evaporation of water requires relatively large amount of energy, either in the form of sensible heat or radiant energy. Therefore, the evapotranspiration process is governed by energy exchange at the vegetation surface and is limited by the amount of energy available. Because of this limitation, it is possible to predict the evapotranspiration rate by applying the principle of energy conservation. In which case, the energy arriving at the surface must equal the energy leaving the surface for the same time period. This energy balance equation can be used for hourly or shorter values especially during daylight hours. The Bowen ratio approach is the most commonly used method. It is the ratio of energy flux from one medium to another by sensible and latent heat respectively. The instrumentation requirements and technical procedures involved generally limit the energy balance method to research studies over relatively short periods of time, but the

result can be very reliable if the measurements are accurate because they are obtained under natural environmental conditions.

The energy balance is given as:

$$R_n - G - \lambda\text{ET} - \text{H} = 0 \quad (2.9)$$

Where; Rn is Net radiation, G is Soil heat flux, H is Sensible heat and λET is Latent heat flux.

2.4.2 Soil water balance method

Moorhead (2018) stressed that with the soil water balance approach, the drainage and runoff terms can be difficult to determine. Also, Evapotranspiration can be determined by measuring the various components of the soil water balance. The method consists of assessing the incoming and outgoing water flux in the crop root zone over some time period. Irrigation [I] and rainfall [P] add water to the root zone. Part of I and P might be lost by surface runoff [RO] and by deep percolation [DP] that will eventually recharge the water table. Water might also be transported upward by capillary rise (CR) from a shallow water table towards the root zone or even transferred horizontally by subsurface flow in (SFin) or out of (SFout) from the root zone. In many situations, however, except under conditions with large slopes, SFin and SFout are minor and can be ignored.

$$ET = I + \text{P} - \text{RO} - \text{DP} + \text{CR} \pm \Delta\text{SF} \pm \Delta\text{SW} \quad (2.10)$$

Soil evaporation and crop transpiration deplete water from the root zone. If all fluxes other than evapotranspiration [ET] can be assessed, the transpiration can be deduced from the change in soil water content (ΔSW) over the period.

2.4.3 Lysimeter method

By isolating the crop root zone from its environment and controlling the processes that are difficult to measure, the different terms in the soil water balance equation can be

determined with greater accuracy. This is done in lysimeters where the crop grows in isolated tanks filled with either disturbed or undisturbed soil. In precision weighing lysimeters, where the water loss is directly measured by the change of mass, evapotranspiration can be obtained with a few hundredths of a millimeter; and small time periods such as hour can be considered. In non-weighing lysimeters the evapotranspiration for a given time period is determined by deducting the drainage water, collected at the bottom of the lysimeters, from the total input. Thus in using lysimeters, such occurrences like deep percolation and upward capillary rise from shallow water table are eliminated since the lysimeter is a barrier to these problems. Therefore, equation (2.10) can be reduced as given in equation (2.11). (input – output = change in storage (ΔS). For quantification of evapotranspiration, the equation is written as:

$$ET_C = P + \mathrm{I} - \mathrm{D} - \mathrm{R} - \Delta S \qquad (2.11)$$

Where, ETc is Crop evapotranspiration ($mmday^{-1}$)

P is Rainfall (mm)

D is Drainage (mm)

I is Irrigation (mm)

Δ is Water drained (mm)

ΔS is Change in the soil water

CHAPTER THREE

3.0 MATERIALS AND METHODS

3.1 Study Area

Minna is located between 9.68 ^{0}N and 6.50 ^{0}E. The average annual temperature and rainfall were 27.5 ^{0}C and 1229 mm respectively (Kuti *et al*., 2018). Shiroro is located on between 9.98 ^{0}N and 6.80 ^{0}E. Bida is located between 9.08 ^{0}N and 6.00 ^{0}E. Temperature is high in the period of dry season and less in full wet raining season between 27 °C and 35 °C (Kuti *et al*., 2016).

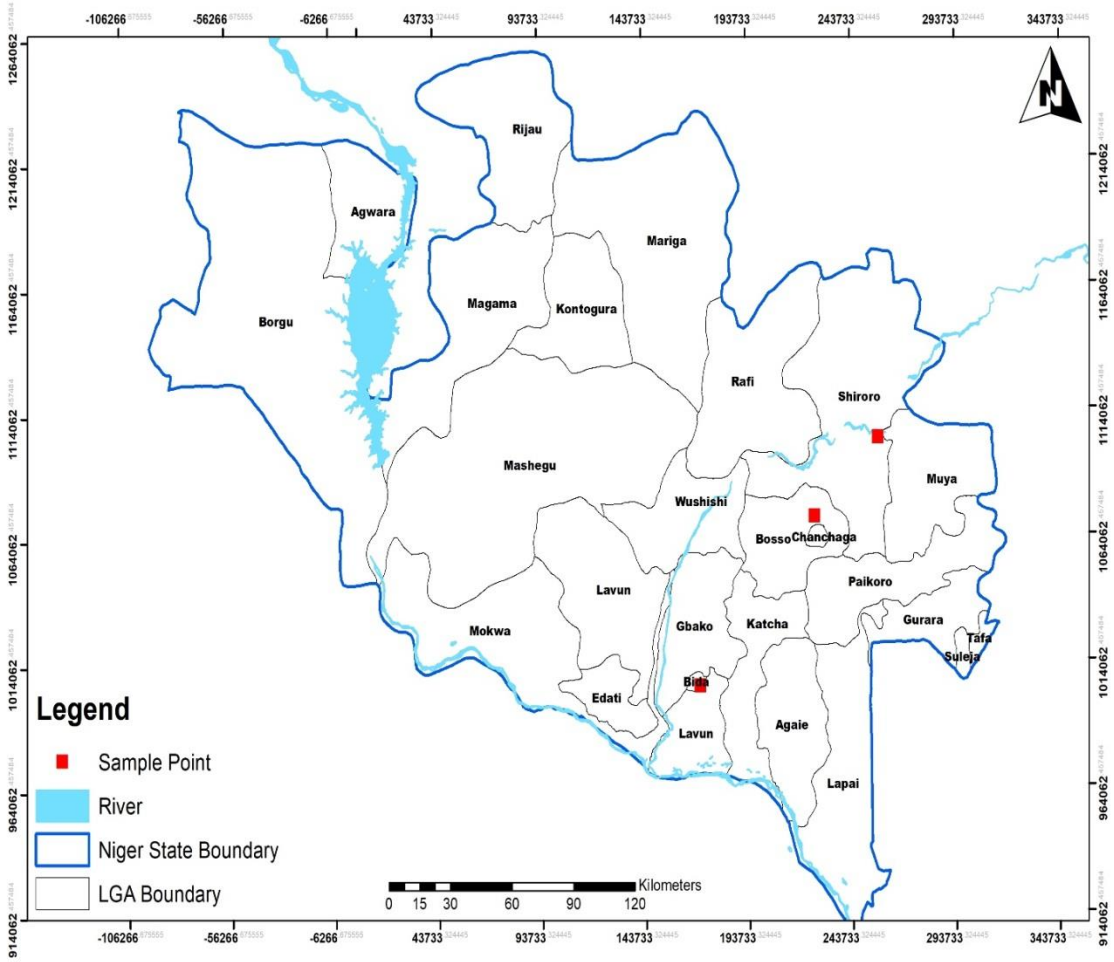

Figure 3.1: Map of the study area

3.2 Data Used

National Aeronautics and Space Administration (NASA), through its Earth Science research program, has long supported satellite systems and research providing data important to the study of climate and climate processes (Chandler *et al.*, 2004). NASA collected monthly averages of environmental data such as solar radiation, minimum and maximum temperature, relative humidity, and wind speed at 2 metres. Thirty eight years (1982 -2020) records were obtained from NASA for this investigation. These data include long-term climatologically averaged estimates of meteorological quantities and surface solar energy fluxes. Additionally, mean daily values of the base meteorological and solar data are provided in time series format (Chandler *et al.,* 2004). These satellite and model-based products have been shown to be sufficiently accurate to provide reliable solar and meteorological resource data over regions where surface measurements are sparse or non-existent (Chandler *et al.*, 2004).

All parameters are available on a 0.5° x 0.5° latitude and longitude global grid. All the Meteorological parameters were derived from the NASA's GMAO MERRA-2 assimilation model (Bloom *et al.,* 2005; Bai *et al.,* 2010). Ohunakin *et al.* (2015) reported that meteorological data from NASA observation gave a better performance than Nigerian Meteorological Agency (NIMET) because of the wider coverage of data reading across Nigeria.

3.3 Determination of Reference Evapotranspiration (RET) Using Penman-Monteith

The reference evapotranspiration (RET) was determined using the procedure outlined by Zotarelli *et al*. (2010). The equation 3.1 was used to determine RET.

$$ET_O = \frac{0.408\,\Delta\,(R_n - G) + \gamma\left[\frac{900}{T+273}\right]U_2\,(e_s - e_a)}{\Delta + \gamma\,(1.0 + 0.34\,U_2)} \qquad (3.1)$$

where ET_o (mm/d) is the reference evapotranspiration; Δ (kPa $(^oC)^{-1}$) is the slope of the saturation vapour pressure; R_n (MJ/m^2day) stands for net radiation term; G (MJ $m^{-2}day^{-1}$) is sensible heat flux into the soil; T (^oC) stands for average air temperature; U_2 (ms^{-1}) represents wind speed taken at the height of 2 m; $e_s - e_a$ (kPa) represents the vapour pressure deficit in the air; γ (kPa$(^oC)^{-1}$) stands for the psychometric constant.

3.4 Step by Step Procedure used to determine Reference Evapotranspiration

Step 1 – Mean daily temperature

$$\boldsymbol{T_{mean}} = \frac{\boldsymbol{T_{max}} + \boldsymbol{T_{min}}}{\mathbf{2}} \quad (3.2)$$

where,

$\boldsymbol{T_{mean}}$ = mean daily air temperature, °C;

$\boldsymbol{T_{max}}$ = maximum daily air temperature, °C;

$\boldsymbol{T_{min}}$ = minimum daily air temperature, °C;

Step 2 – Mean daily solar radiation (R_s)

$$Rs_{(\mathrm{MJ\ m} - 2_{\mathrm{day}} - 1)} = R_{s(\mathrm{W\ m} - 2_{\mathrm{day}} - 1)} * 0.0864 \quad (3.3)$$

Step 3 – Wind speed (u_2)

$$u_2 = u_h \frac{4.87}{ln\,(67.8\,h - 5.42)} \quad (3.4)$$

where,

u2 = wind speed 2 m above the ground surface, m s^{-1};

uz = measured wind speed z m above the ground surface, m s^{-1};

h = height of the measurement above the ground surface, m.

$u_{2(m\,s} - 1) = u2\ (mi\ h^{-1}) * 0.447$

Step 4 - Slope of saturation vapor pressure curve (î)

$$\Delta = \frac{4098\left[0.6108 exp\left(\frac{17.27 * T_{mean}}{T_{mean} + 237.3}\right)\right]}{(T_{mean} + 237.3)^2} \quad (3.5)$$

T_{mean} = mean daily air temperature

exp = 2.7183 (base of natural logarithm).

Step 5 – Atmospheric Pressure (P)

$$P = 101.3 \left[\frac{293 - 0.0065z}{293}\right]^{5.26} \quad (3.6)$$

where,

z = elevation above sea level, m.

Step 6 – Psychrometric constant (³)

$$\gamma = \frac{C_p P}{\varepsilon \lambda} = 0.000665\ P \quad (3.7)$$

where

³ = psychrometric constant, kPa °C-1;

P = atmospheric pressure, kPa;

ª = latent heat of vaporization, 2.45, MJ kg-1;

c_p = specific heat at constant pressure, 1.013 10-3, MJ kg-1 °C^{-1};

Step 7 – Delta Term (DT) (auxiliary calculation for Radiation Term)

$$\boldsymbol{DT} = \frac{\Delta}{\Delta + \boldsymbol{\gamma}\,(\mathbf{1} + \mathbf{0.34}\,\boldsymbol{u_2})} \quad (3.8)$$

where,

Δ = slope of saturation vapor curve;

γ = psychrometric constant, kPa °C-1;

u2 = wind speed 2 m above the ground surface, m s-1.

Step 8 – Psi Term (PT) (auxiliary calculation for Wind Term)

$$\boldsymbol{PT} = \frac{\Delta}{\Delta + \boldsymbol{\gamma}\,(\mathbf{1}+\mathbf{0.34}\,\boldsymbol{u_2})} \tag{3.9}$$

where,

Δ = slope of saturation vapor curve;

γ = psychrometric constant, kPa °C-1;

u_2 = wind speed 2 m above the ground surface, m s-1.

Step 9 – Temperature Term (TT) (auxiliary calculation for Wind Term)

$$\boldsymbol{TT} = \left[\frac{\mathbf{900}}{\boldsymbol{T_{mean}} + \mathbf{273.3}}\right] * \boldsymbol{u_2} \tag{3.10}$$

where,

T_{mean} = mean daily air temperature, ºC.

u_2 = wind speed 2 m above the ground surface, m s-1.

Step 10 -Mean saturation vapor pressure derived from air temperature (e_s)

$$e(T) = 0.6108exp\left[\frac{17.27T}{T+237.3}\right] \tag{3.11}$$

where, e(T) = saturation vapor pressure at the air temperature T, kPa

T = air temperature, ºC.

Step 11 – Actual vapor pressure (ea) derived from relative humidity

$$\boldsymbol{e_a} = \frac{\boldsymbol{e}_{(T_{min})}\left[\frac{\boldsymbol{RH_{max}}}{\mathbf{100}}\right] + e(T_{max})\left[\frac{\boldsymbol{RH_{min}}}{\mathbf{100}}\right]}{\mathbf{2}} \tag{3.12}$$

where,

e_a = actual vapour pressure, kPa;

$e_{(T_{min})}$ = saturation vapour pressure at daily minimum temperature, kPa;

$e_{(T_{max})}$ = saturation vapour pressure at daily maximum temperature, kPa;

RH_{max} = maximum relative humidity, %;

RH_{max} = minimum relative humidity, %;

Step 12 – The inverse relative distance Earth-Sun (dr) and solar declination (¥)

$$d_r = 1 + 0.033cos\left[\frac{2\pi}{365}\ J\right] \quad (3.13)$$

$$\delta = 0.409sin\left[\frac{2\pi}{365}\ J - 1.39\right]$$

where,

J = number of the day in the year between 1 (1 January) and 365 or 366 (31 December).

Step 13 – Conversion of latitude (Æ) in degrees to radians

$$\varphi\ [Radians] = \frac{\pi}{180}\ \varphi\ [decimal\ degrees] \quad (3.14)$$

e.g.1. to convert 13º44N to decimal degrees = 13+44/60 = 13.73

e.g.2. to convert 22º54S to decimal degrees = (-22)+(-54/60) = -22.90

Step 14 - Sunset hour angle (…s)

The sunset hour angle is given by:

$$\omega_s = arccos\ [-tan\ (\varphi)tan\ (\delta)] \quad (3.15)$$

Where,

Æ = latitude expressed in radians;

¥ = solar declination;

φ = radians

Step 15 – Extraterrestrial radiation (Ra)

$$R_a = \frac{24(60)}{\pi}\ G_{sc}d_r\ [(\omega_s\ sin\ \varphi\ sin\ \delta) + (\cos\ \varphi\ cos\ \delta\ sin\ \omega_s)] \quad (3.16)$$

where,

R_a = extraterrestrial radiation, MJ m-2 day-1;

G_{SC} = solar constant = 0.0820 MJ m-2 min-1;

dr = inverse relative distance Earth-Sun;

ω_s = sunset hour angle, rad;

Æ = latitude, rad;

¥ = solar declination, rad.

Step 16 – Clear sky solar radiation (Rso)

The calculation of the clear-sky radiation is given by:

$$R_{so} = (0.75 + 2E10^{-5}z)R_a \quad (3.17)$$

where,

z = elevation above sea level, m;

R_a = extraterrestrial radiation, MJ m^{-2} day^{-1};

Step 17 – Net solar or net shortwave radiation (Rns)

$$R_{ns} = (1 - a)R_s \quad (3.18)$$

where,

R_{ns} = net solar or shortwave radiation, MJ m^{-2} day^{-1};

± = albedo or canopy reflection coefficient, which is 0.23 for the hypothetical grass reference crop, dimensionless;

R_s = the incoming solar radiation, MJ m-2 day-1;

Step 18 – Net outgoing long wave solar radiation (Rnl)

The rate of longwave energy emission is proportional to the absolute temperature of the surface raised to the fourth power. This relation is expressed quantitatively by the Stefan-Boltzmann law. The net energy flux leaving the earth's surface is, however, less than that emitted and given by the Stefan-Boltzmann law due to the absorption and downward radiation from the sky. Water vapor, clouds, carbon dioxide and dust are absorbers and emitters of longwave radiation. It is thereby assumed that the concentrations of the other absorbers are constant:

$$R_{nl} = \sigma \left[\frac{(T_{max}+273.16)^4+(T_{min}+273.16)^4}{2}\right](0.34 - 0.14\sqrt{e_a})\left[1.35\frac{R_s}{R_{so}} - 0.35\right] \quad (3.19)$$

where,

R_{nl} = net outgoing longwave radiation, MJ m^{-2} day^{-1},

¥ = Stefan-Boltzmann constant [4.903 10^{-9} MJ K^{-4} m^{-2} day^{-1}],

T_{max} = K maximum absolute temperature during the 24-hour period [K = °C + 273.16],

T_{min} = K minimum absolute temperature during the 24hour period [K = °C + 273.16],

e_a = actual vapor pressure, kPa,

R_s = the incoming solar radiation, MJ m-2 day-1;

R_{so} = clear sky solar radiation, MJ m-2 day-1;

Step 19 – Net radiation (Rn)

$R_n = R_{ns} - R_{nl}$ (3.20)

where,

R_{ns} = net solar or shortwave radiation, MJ m-2 day^{-1};

R_{nl} = net outgoing longwave radiation, MJ m^{-2} day^{-1}.

To express the net radiation (R_n) in equivalent of evaporation (mm) (R_{ng});

R_{ng} = 0.408 X Rn Where, Rn = net radiation, MJ m-2 day-^{1};

Final Step – Overall ETo equation

FS1. Radiation term (ET_{rad})

$$ET_{rad} = DT\ X\ R_{ng}$$

where,

ET_{rad} = radiation term, mm d^{-1};

DT Delta term;

R_{ng} = net radiation, mm,

FS2. Wind term (ET_{wind})

$$ET_{wind} = PT\ X\ TT\ (e_s - e_a)$$

where,

ET_{wind} = wind term, mm d^{-1};

PT = Psi term;

TT = Temperature term;

e_a = actual vapor pressure, kPa;

e_s = mean saturation vapor pressure derived from air temperature, kPa;

Final Reference Evapotranspiration Value (ET_o)

$$ET_o = ET_{wind} + ET_{rad}$$

where,

ET_o = reference evapotranspiration, mm d^{-1};

ET_{wind} = wind term, mm d^{-1};

ET_{rad} = radiation term, mm d^{-1};

3.5 Trend Analysis for Reference Evapotranspiration

3.5.1 Mann-kendal test

The study explored Mann-Kendall statistic for monthly RET records, and Kendall tau statistic, τ, to test for randomness against trend in reference evapotranspiration (Kuti *et al*., 2016). In this test, the null hypothesis Ho states that the deseasonalized data ($x_1 \ldots x_n$) are a sample of n independent and identically distributed random variables. The alternative hypothesis H_1 of a two-sided test is that the distribution of x_k and x_j is not identical for all $k, j \leq n$ with $k \neq j$. The variance (S) was calculated with equation 3.21 and 3.22, has mean zero:

$$Var(S) = [n(n-1)(2n+5) - \sum_t t\,(t-1)(2t+5)]/18 \quad (3.21)$$

$$S = \sum_{K=1}^{n-1} \sum_{j=k+1}^{n} Sgn(x_j - x_k) \quad (3.22)$$

$$Sgn(x_j - x_k) = \begin{cases} +1 & if\ (x_j - x_k) > 0 \\ 0 & if\ (x_j - x_k) = 0 \\ -1 & if\ (x_j - x_k) < 0 \end{cases} \quad (3.23)$$

and is asymptotically normal, where *t* is the extent of any given tie, and *t* denotes the summation over all ties. For the cases in which *n* is larger than 10, the standard normal variate Z is computed by using the following equation (Kuti *et al*., 2016; Ewemoje & Umego, 2018):

$$Z = [\begin{cases} \frac{S-1}{\sqrt{Var(S)}} & \begin{cases} if & S > 0 \\ if & S = 0] \end{cases} \\ \frac{S+1}{\sqrt{Var(S)}} & if \quad S < 0 \end{cases} \quad (3.24)$$

The test statistic Zs was used as a measure of significance of trend. In fact, this test statistic was also used to test the null hypothesis, $H0$: There is no monotonic trend in the data. If Zs is greater than $Z\propto$ 2, where represents the chosen significance level (usually 5%, with $Z_{0.025}$= 1.96), then the null hypothesis is invalid, meaning that the trend is significant.

3.6 Multiple Linear Regression Model

The study explored linear regression to assess the factors causing either decreasing or increasing trend reference evapotranspiration in the three locations. The response variable is RET, while the independent variables are mean temperature, Mean saturation on vapour pressure, actual vapour pressure, net radiation, psychometric constant, wind speed and slope of saturated vapour pressure. All linear assumptions were determined to test the validity of the result.

$$y_i = \beta_0 + \sum_{j-1}^{p} \beta_j\, x_{ij} + \varepsilon_i \quad (3.25)$$

y_i is the dependent or predicted variable

x_{ij} are the regression coefficient representing the change in y relative to a one-unit change in x_{ij}

ε_i is the model's random error (residual) term.

J is the observation in row number.

I is the standardized regression coefficient.

The software used for the analysis is XLSTAT 2015 version. Best model was used to handle a number of variable. The reason for choosing it was to select several criteria to determine the best model, which include adjusted R^2 mean square of error (MSE).

3.7 Sen's Slope

To estimate the true slope of an existing trend (as change per year) the Sen's nonparametric method is used. The Sen's method can be used in cases where the trend can be assumed to be linear. This means that *f(t)* is equal to

$$f(t) = Qt + B \tag{3.26}$$

Where

Q is the slope and B is a constant.

To get the slope estimate *Q* in equation (3.26) we first calculate the slopes of all data value pairs

$$Q_i = \frac{x_i - x_i}{j-k} \tag{3.27}$$

where

j>k.

If there are *n* values *xj* in the time series we get as many as *N = n(n-1)/2* slope estimates *Qi*.

The Sen's estimator of slope is the median of these *N* values of *Qi*. The *N* values of *Qi* are ranked from the smallest to the largest and the Sen's estimator is

$$Q = Q\,[(N+1)/2]\ ,\ \textit{if } N \textit{ is odd} \tag{3.28}$$

or

$$Q = \frac{1}{2}(Q_{\,[N/2]} + Q_{\,[(N/2)/2]}),\ \text{if } N \text{ is even.}$$

CHAPTER FOUR

4.0 RESULTS AND DISCUSSION

4.1 Determination of Reference Evapotranspiration in Selected Areas in Niger State

4.1.1 Determination of reference evapotranspiration in Minna

Table 4.1 shows the reference evapotranspiration in Minna. The minimum and maximum RETs ranges from 1.40 and 3.11; 2.01 and 7.49 mm/day. The lowest average value was 1.40 in August and the highest value of 3.11 mm/day was in January. 0.08 was the lowest standard deviation in September with the highest value of 1.02 (February). The coefficient of variation (CV) varies between 8.5% and 36.03 in June and February. The comprehensive data of the RET over 1982-2020 is shown in Appendix I.

Table 4.1: Descriptive statistic of Minna reference evapotranspiration

Month	Minimum	Maximum	Mean	Standard deviation	CV (%)
Jan	3.11	6.56	3.11	0.95	30.47
Feb	2.84	7.49	2.84	1.02	36.03
Mar	2.77	6.09	2.77	0.77	27.95
Apr	2.39	4.75	2.39	0.56	23.33
May	1.98	3.55	1.98	0.34	17.27
Jun	1.74	2.38	1.74	0.15	8.47
Jul	1.62	2.07	1.62	0.11	7.02
Aug	1.40	2.21	1.40	0.13	9.41
Sep	1.67	2.01	1.67	0.08	4.80
Oct	1.84	2.71	1.84	0.21	11.66
Nov	2.60	4.39	2.60	0.45	17.38
Dec	2.81	5.82	2.81	0.76	27.16

4.1.2 Determination of reference evapotranspiration in Shiroro

The reference evapotranspiration in Shiroro is shown in Table 4.2. The minimum and maximum RETs are 1.36 and 3.76; 2.03 and 9.22 mm/day. August had the lowest average value of 1.36 and the highest value of 3.76 mm/day (January). The lowest standard deviation was 0.10 in September, while the peak was 1.23 (February). The minimum and

maximum coefficients of variation were 6.12 and 35.79 %, respectively in September and February. The comprehensive data of the RET over 1982-2020 is shown in Appendix II.

Table 4.2: Descriptive statistic of Shiroro reference evapotranspiration

Month	Minimum	Maximum	Mean	Std. deviation	CV (%)
Jan	3.76	7.81	3.76	1.09	29.02
Feb	3.49	9.22	3.49	1.23	35.29
Mar	3.17	7.77	3.17	1.14	35.79
Apr	2.53	6.16	2.53	0.72	28.32
May	1.93	3.39	1.93	0.38	19.48
Jun	1.66	2.46	1.66	0.15	9.31
Jul	1.55	2.05	1.55	0.13	8.20
Aug	1.36	2.03	1.36	0.13	9.37
Sep	1.63	2.10	1.63	0.10	6.12
Oct	1.89	2.99	1.89	0.28	14.77
Nov	2.95	5.26	2.95	0.53	18.06
Dec	3.24	7.19	3.24	0.90	27.75

4.1.3 Determination of reference evapotranspiration in Bida

Table 4.3 shows the reference evapotranspiration in Bida 1.57 and 2.92; 2.28 and 5.53 mm/day are the minimum and maximum RET, respectively. The lowest average value was 1.57, and the highest was 2.92 mm/day in August (January). The standard deviation was 0.10 in September and was 0.74 in February. In September and February, the minimum and highest coefficients of variation were 5.51 and 25.59 % respectively. The comprehensive data of the RET over 1982-2020 is shown in Appendix III.

Table 4.3: Descriptive statistic of Bida reference evapotranspiration

Month	Minimum	Maximum	Mean	Standard deviation	CV (%)
Jan	2.92	5.53	2.92	0.70	23.85
Feb	2.88	6.03	2.88	0.74	25.59
Mar	2.85	5.29	2.85	0.60	20.92
Apr	2.62	4.45	2.62	0.51	19.33
May	2.14	3.79	2.14	0.36	16.61
Jun	1.89	2.59	1.89	0.17	9.08
Jul	1.77	2.36	1.77	0.15	8.32
Aug	1.57	2.54	1.57	0.17	10.90
Sep	1.78	2.28	1.78	0.10	5.51
Oct	1.99	2.82	1.99	0.18	9.23
Nov	2.66	4.08	2.66	0.39	14.61
Dec	2.63	5.29	2.63	0.61	23.22

4.2 Trend Analysis Results

4.2.1 Trend analysis of reference evapotranspiration using Mann-kendall in Minna

Table 4.4 shows Minna reference evapotranspiration using the Mann-Kendall statistic. The monthly values of reference evapotranspiration for the period of study 1982-2020, shows an overall increasing trend ranging from Mann-Kendal Test values of 0.605 to 4.137. The monthly RET trend significantly at $p<0.001$ in April (3.411); November (3.6629) and December (4.137); at $p<0.01$ in January (3.024); March (2.879); May (2.710); June (2.734); July (2.879); at $p<0.05$ in February (2.492); September (2.371) and at $P>0.1$ in August (1.621) and October (0.605). The annual monthly reference evapotranspiration had values of Sens slope, which ranges from 0.002 to 0.039. Figure 4.1 also indicated an increase in trend by positive slope value.

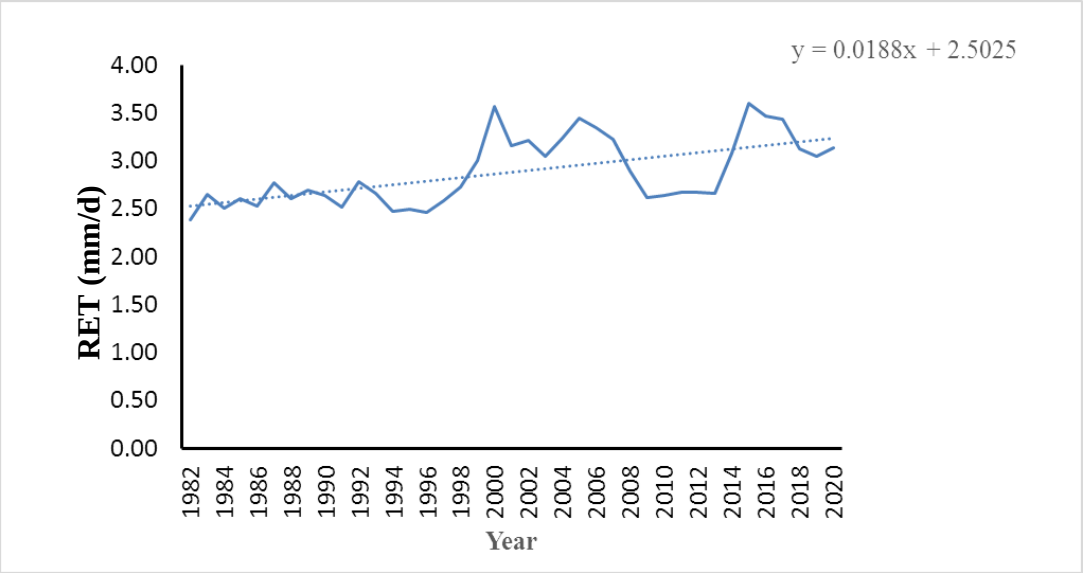

Figure 4.1: Annual reference Evaporation trend for Minna (1982 -2020)

Table 4.4: Reference evapotranspiration in Minna using Mann-Kendall test

	Mann-Kendall trend		Sen's slope estimate
Month	**Test Z**	**Signific.**	**Sen's slope (Q)**
Jan	3.024	**	0.031
Feb	2.492	*	0.037
Mar	2.879	**	0.029
Apr	3.411	***	0.023
May	2.710	**	0.012
Jun	2.734	**	0.005
Jul	2.879	**	0.004
Aug	1.621		0.003
Sep	2.371	*	0.003
Oct	0.605		0.002
Nov	3.629	***	0.020
Dec	4.137	***	0.033

Note: *** trend at 0.001 level of significant; **trend at 0.01 level of significant; * trend at 0.05 level of significant

4.2.2 Trend analysis of reference evapotranspiration using Mann-kendall in Shiroro

Table 4.5 shows Shiroro RET using the Mann-Kendal statistic. The monthly values of RET for the period of study 1982-2020, shows an overall increasing trend ranging from Z values of 0.556 to 4.137, the monthly RET trend significantly at $p<0.001$ in June (3.532); and December (3.363); at $p<0.01$ in January (2.927); April (2.613); March

(2.879); July (2.879); September (2.879); and November (2.806). At p<0.05 February (2.129); March (2.153) and May (2.226). At P>0.1 in August (1.500) and October (0.556). The annual monthly reference evapotranspiration had Sens's slope values, which range from 0.003 to 0.037. Figure 4.2 indicated an increase in trend by positive slope value.

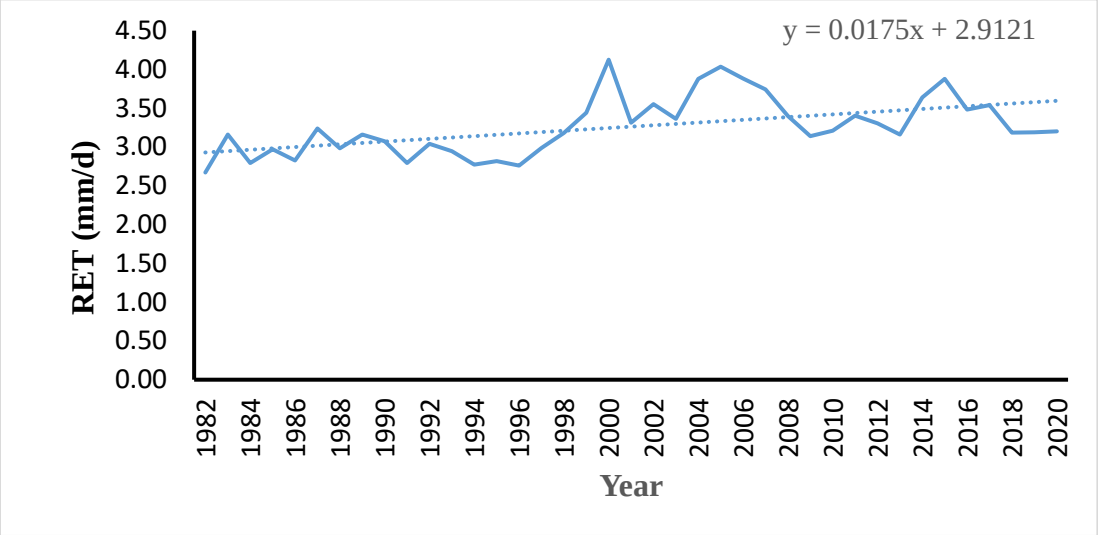

Figure 4.2 : Annual reference evaporation trend for Shiroro (1982 -2020)

Table 4.5: Reference evapotranspiration in Shiroro using Mann-Kendall test

	Mann-Kendall trend		**Sen's slope estimate**
Month	**Test Z**	**Signific.**	**Sen's slope (Q)**
Jan	2.927	**	0.034
Feb	2.129	*	0.037
Mar	2.153	*	0.031
Apr	2.613	**	0.019
May	2.226	*	0.008
Jun	3.532	***	0.007
Jul	2.686	**	0.005
Aug	1.500		0.003
Sep	2.879	**	0.005
Oct	0.556		0.003
Nov	2.806	**	0.014
Dec	3.363	***	0.028

Note: *** trend at 0.001 level of significant; **trend at 0.01 level of significant; * trend at 0.05 level of significant

4.2.3 Trend analysis of reference evapotranspiration using Mann-Kendall in Bida

Table 4.6 shows Bida RET using the Mann-Kendall statistic. The annual RET for 39 years shows an overall increasing trend ranging from Z values of 1.028 to 4.174. The monthly reference evapotranspiration trend is significant at $p<0.001$ in March (3.472); November (4.174) and December (4.004); at $p<0.01$ in April (3.133). At $p<0.05$ in January (2.407); February (2.359); May (2.480); June (2.045); July (2.359) and August (2.020). At $P>0.1$ in September (0.980) and October (1.028). The Sens's slope ranges from 0.00 to 0.029 mm/year. Figure 4.3 indicated an increase in trend by positive slope value.

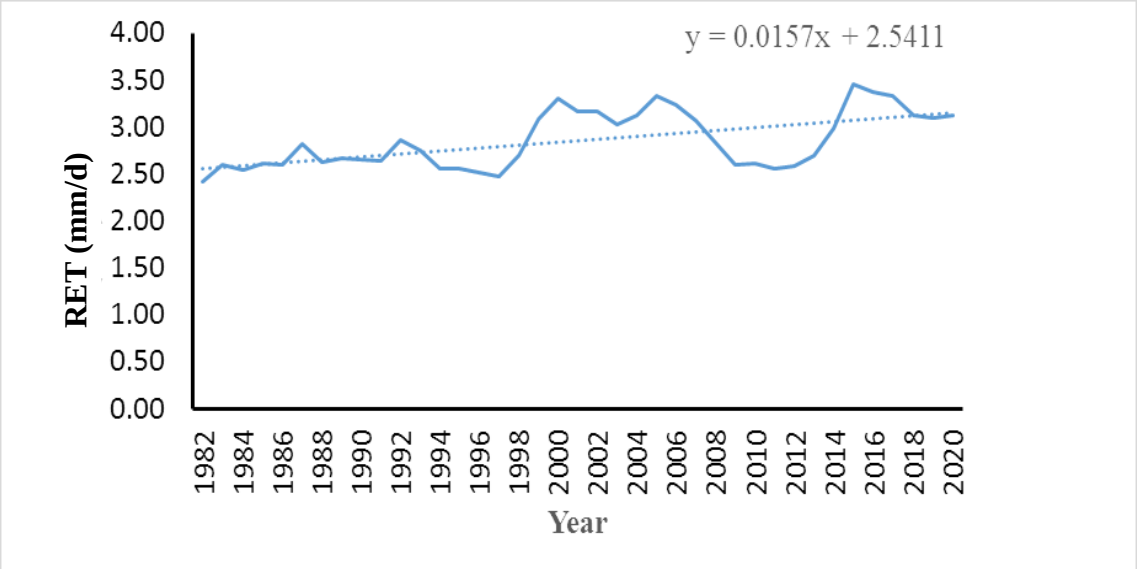

Figure 4.3: Annual reference evapotranspiration trend for Bida (1982 -2020)

Table 4.6: Reference evapotranspiration in Bida using Mann-Kendall test

	Mann-Kendall trend		Sen's slope estimate
Time series	**Test Z**	**Signific.**	**Sen's slope (Q)**
Jan	2.407	*	0.026
Feb	2.359	*	0.029
Mar	3.472	***	0.026
Apr	3.133	**	0.022
May	2.480	*	0.013
Jun	2.045	*	0.006
Jul	2.359	*	0.004
Aug	2.020	*	0.003
Sep	0.980		0.002
Oct	1.028		0.002
Nov	4.174	***	0.017
Dec	4.004	***	0.026

Note: *** trend at a 0.001 level of significant; **trend at a 0.01 level of significant; * trend at a 0.05 level of significant.

4.3 Assessment of the Factors Influencing Reference Evapotranspiration in Selected Areas in Niger State

4.3.1 Assessment of the factors influencing reference evapotranspiration in Minna

Table 4.7 shows the goodness of fit for annual reference evapotranspiration. The relationship between the independent variables (Temperature (mean), Psychometric constant, Mean Saturation Vapour Pressure (es), Actual Vapour Pressure (ea), Slope of SVP, Net Radiation, Wind Speed at 2 m and RET was linear and had a strong coefficient of determination (R^2=0.96532). The values of adjusted R^2 and mean square error (MSE) were 0.96531 and 0.048. Durbin Watson (DW) had a value of 0.745.

Table 4.7: Goodness of fit statistics for daily annual RET

Statistical tools	**Values**
Observations (n)	14245
Sum of weights	14245.000
DF	14238.000
R^2	0.96532
Adjusted R^2	0.96531
MSE	0.048
RMSE	0.220
DW	0.745

Table 4.8 shows Minna reference evapotranspiration's model parameters. The mean saturation Vapour pressure had a value of 1.398 followed by wind speed at 2m (0.612), average temperature (0.609), net radiation of (0.279) and was statistically significant ($p<0.05$). The actual vapour pressure and slope of saturated vapour pressure have values of -1.215 and -65.377. The psychometric constant shows a negligible value. All the factors were statistically significant except psychometric constants.

Table 4.8: Model parameters of RET in Minna

Source	Value	Standard error	t	Pr > |t|	Lower bound (95%)	Upper bound (95%)
Intercept	-4.593	0.092	-50.031	< 0.0001	-4.773	-4.413
Temperature (mean)	0.609	0.012	51.097	< 0.0001	0.586	0.633
Psychometric constant	0.000	0.000				
Mean Saturation Vapour Pressure (es)	1.398	0.037	37.601	< 0.0001	1.325	1.471
Actual Vapour Pressure (ea)	-1.215	0.009	-137.925	< 0.0001	-1.232	-1.198
Slope of SVP	-65.377	1.405	-46.518	< 0.0001	-68.131	-62.622
Net Radiation	0.279	0.002	146.712	< 0.0001	0.275	0.282
Wind Speed at 2m	0.612	0.004	165.763	< 0.0001	0.605	0.619

The RET model is as shown in equation 4.1 for Minna.

$$\text{RET} = -4.593 + 0.609\,\text{Tmean} + 1.398(\text{es}) - 1.215(\text{ea}) - 65.377\,\text{SVP} + 0.279\text{Rn} + 0.612\,U_2 \quad (4.1)$$

4.3.2 Assessment of the factors influencing reference evapotranspiration in Shiroro

Table 4.9 shows the goodness of fit for daily annual reference evapotranspiration. The relationship between the factors and RET is linear, with a strong coefficient of determination (0.97055). The values of adjusted R^2, MSE were 0.97054 and 0.080. Durbin Watson (DW) value was 0.751 for Shiroro RET.

Table 4.9: Goodness of fit statistics for Shiroro daily annual RET

Statistical tools	Values
Observations (n)	14245
Sum of weights	14245.000
DF	14238.000
R^2	0.97055
Adjusted R^2	0.97054
MSE	0.080
RMSE	0.284
DW	0.751

Table 4.10 shows model parameters for Shiroro reference evapotranspiration. The average temperature (Tmean), wind speed at 2m, mean saturation vapour pressure and net radiation had values of 0.986, 0.647, 0.533, and 0.243, while the actual vapour pressure and slope of saturated vapour pressure have a value of 1.746 and -80.979. The psychometric has a negligible value in Shiroro. All the factors were statistically significant except psychometric constants.

Table 4.10: Shiroro RET Model parameters

Source	Value	Standard error	t	Pr > |t|	Lower bound (95%)	Upper bound (95%)
Intercept	-6.770	0.109	-62.140	< 0.0001	-6.983	-6.556
Tmean	0.986	0.016	60.502	< 0.0001	0.954	1.018
Psychometric constant	0.000	0.000				
Mean Saturation Vapour Pressure (es)	0.533	0.053	10.002	< 0.0001	0.429	0.638
Actual Vapour Pressure (ea)	-1.746	0.012	-149.058	< 0.0001	-1.769	-1.723
Slope of SVP	-80.979	2.083	-38.880	< 0.0001	-85.062	-76.897
Net Radiation	0.243	0.002	109.920	< 0.0001	0.239	0.248
Wind Speed at 2m	0.647	0.004	175.579	< 0.0001	0.640	0.654

The Shiroro RET model is as shown in equation 4.2.

$$\text{RET} = -6.770 + 0.986\text{Tmean} + 0.533(\text{es}) - 1.746\ (\text{ea}) - 80.979\ \text{SVP} + 0.243\ \text{Rn} + 0.647\text{U}_2 \quad (4.2)$$

4.3.3 Assessment of the factors influencing reference evapotranspiration in Bida

Table 4.11 shows the goodness of faith for daily annual reference evapotranspiration. The relationship between the independent variables and dependent variables (RET) is linear and had a strong coefficient of determination (0.96274), the values of R^2, MSE, DW were 0.96272, 0.034 and 0.934, respectively.

Table 4.11: Goodness of fit statistics for Bida daily annual RET

Statistical tools	Varies
Observations (n)	14245
Sum of weights	14245.000
DF	14238.000
R^2	0.96274
Adjusted R^2	0.96272
MSE	0.034
RMSE	0.184
DW	0.934

Table 4.12 shows Bida RE Model parameters. The mean saturation Vapour pressure had high impact on reference evapotranspiration (1.544) followed by wind speed at 2m (0.559), net radiation of (0.300); they were statistically significant ($p<0.05$). The actual vapour pressure with (-0.947) and slope of saturated vapour pressure of (-35.713). All the factors were statistically significant except psychometric constants.

Table 4.12: Model parameters for Bida RET

Source	Value	Standard error	t	Pr > |t|	Lower bound (95%)	Upper bound (95%)
Intercept	-2.160	0.085	-25.425	< 0.0001	-2.327	-1.994
Tmean	0.239	0.011	22.389	< 0.0001	0.218	0.260
Psychrometric constant	0.000	0.000				
Mean Saturation Vapour Pressure (es)	1.544	0.031	49.939	< 0.0001	1.483	1.604
Actual Vapour Pressure (ea)	-0.947	0.007	-131.699	< 0.0001	-0.962	-0.933
Slope of SVP	-35.713	1.243	-28.740	< 0.0001	-38.149	-33.277
Net Radiation	0.300	0.002	179.131	< 0.0001	0.297	0.304
Wind Speed at 2m	0.559	0.003	160.336	< 0.0001	0.552	0.566

The Bida RET model is as shown in equation 4.3.

$$\text{RET} = -2.160 + 0.239\text{Tmean} + 1.544(\text{es}) - 0.947\ (\text{ea}) - 35.713\text{SVP} + 0.300\text{Rn N} + 0.559\ \text{U}_2 \quad (4.3)$$

4.4 Estimated Reference Evapotranspiration in the Selected Areas in Niger State

Minna had a minimum RET value of 1.4 in August, the Maximum RET of 7.49 in February, which implies that reference evapotranspiration lower in August. The findings agree with existing studies of the analysis of reference evapotranspiration; case study of Asaba and Uyo, south- south Nigeria (Du *et al*., 2016; Ewemoje & Umego, 2018). The coefficient of variation decreases from April to September and increases from October to February for Minna RET. It also decreases again in March. The implication is that reference evapotranspiration is low in the rainy season and was high in the dry seasons. The findings agreed with previous works (Audu *et al.,* 2015) and disagree with similar study (Costa *et al*., 2010).

Shiroro RET has a minimum value of 1.36 in August, the Maximum RET was found in February (9.22) which implies that RET increases in January. The coefficient of variation decreases from April to September over the period for shiroro RET, which implies that, the lowest value was recorded in the month of raining season. The implication is that reference evapotranspiration reduces in the rainy season and was high in the dry seasons. The finding agreed with previous works (Ahmadi & Javanbakht, 2020; Ewemoje & Umego 2018; Audu *et al*., 2015) and disagree with similar study (Costa *et al*., 2010).

Bida RET has a minimum of 1.57 in August, the Maximum RET was found in February (6.03) which implies that RET increases in January. The Bida RET had coefficient of variation that decreases from April to October over the period, which implies that the Bida RET increases from November to March, also fluctuates between August and

October. The implication is that reference evapotranspiration reduces in the rainy season and was high in dry seasons. The finding agreed with previous works (Ahmadi & Javanbakht, 2020; Ewemoje & Umego 2018; Audu *et al*., 2015) and disagree with similar study (Costa *et al*., 2010) at Federal University of Vicosa, Brazil.

4.5 Observed Trend and Changes in RET

In the three study locations, the trend is increasing between 1982 and 2020. The positive trend is more pronounced in different months: Minna (April, November and December), Shiroro (June and December) and Bida (March, November and December). This shows degree of the trend of RET in the selected locations are not the same. This finding is in line with the existing study (Ewemoje & Umego, 2018). Between the end of dry season and early rainy season RET are statistically significant for three locations ($P<0.01$). Although, the trend of Minna and Shiroro are similar in the August and October as both location experienced trends that are positive but not significant.

The trends of RET in September and February are the same and implies soil dryness in Minna. Due to the similarity of the RET trends in April, July, and September with January, Shiroro may experience soil dryness and improper crop growth. RET trends in May, June, July, and August are similar to January and February in Bida. There may be soil moisture loss and improper crop growth, affecting agricultural yield.

4.6 Factors Affecting RET in the Selected Areas in Niger State

The independent variables such as average temperature, actual vapour pressure, net radiation, wind speed at 2m, actual vapour pressure, the slope of saturation vapour pressure, mean saturation vapour pressure change in Minna, Shiroro and Bida RET with R^2 of 0.96532, 0.97054 and 0.96274. The implication is that a strong relationship existed between RET and independent variables in the three locations.

In Minna, the mean saturated vapour pressure had the highest impact on RET followed by wind speed at 2 m and average temperature, while the actual vapour pressure and slope saturated vapour pressure had a negative effect on RET. In Shiroro, the average temperature had the highest impact on RET followed by wind speed at 2 m, while the actual vapour pressure and slope saturated vapour pressure had a negative effect on RET.

In Bida, mean saturated vapour pressure had the highest impact on RET followed by wind speed at 2 m, while the actual vapour pressure and slope saturated vapour pressure had a negative effect on RET. It shows that actual vapour pressure and slope saturated vapour pressure decreased RET in Minna. Shiroro and Bida. The findings disagree with the existing study (Wang *et al*., 2012). The main contributors to the increasing trends of RET in Minna, Shiroro and Bida are mean saturated vapour pressure and average temperature, which is the aerodynamic factor. The findings agree with existing studies (Du *et al*., 2016; Ewemoje & Umego, 2018). The net radiation also changes the trend of RET in Minna, Shiroro and Bida. The outcome disagrees with existing study of Ewemoje & Umego (2018), at Asaba and Uyo, Nigeria.

CHAPTER FIVE

5.0 CONCLUSION AND RECOMMENDATIONS

5.1 Conclusions

The study determined RET and its trends as well as factors causing RET in each location. Reference evapotranspiration varies from one location to another, which could affect irrigation planning and water management in Minna, Shiroro and Bida. The results showed that August had the lowest RET (in 1994) and was highest in February (in 2000). The outcome of this study shows that the trends of RET in each location were increasing and statistically significant. The study concluded that the trend of RET was higher in Shiroro followed by Minna and Bida. The findings indicate that mean saturated vapour pressure followed by average temperature were the major factor responsible for the increasing trends of RET in Minna, Shiroro and Bida. The study concluded that both aerodynamic and net radiation are the major factors influencing increasing trends of RET in Minna, Shiroro and Bida.

5.2 Recommendations

The following recommendations were made from the findings:

(i) Deforestation and bush burning be discouraged in the three locations of study.

(ii) Planting of trees should be encouraged in the three selected areas of study.

(iii) The future work should incorporate net water requirement for major crops in the selected locations.

5.3 Contribution to Knowledge

The study contributed to knowledge by establishing that aerodynamic and Net Radiation are the major factors influencing the trends of Reference Evapotranspiration in the selected areas in Niger State.

REFERENCES

Ahmadi, S. H. & Javanbakht, Z. (2020). Assessing the physical and empirical reference evapotranspiration (RET) models and time series analyses of the influencing weather variables on RET in a semi-arid area. *Journal of Environmental Management*, 276, 111-278.

Allen, R. G., Pereira, L. S., Raes, D. & Smith, M. (1998). Crop evapotranspiration-Guidelines for computing crop water requirements-FAO. Irrigation and drainage paper 56. *FAO, Rome.* 300(9), 87-210.

Allen, R. G., Pereira, L. S., Raes, D. & Smith, M. (2006). Crop Evapotranspiration: guidelines for Computing Crop Water Requirements. FAO-56, Rome.

Allen, R., Tasukmi, M. & Trezza, R. (2007). Satellite-based energy balance for mapping evapotranspiration with internalized calibration (METRIC)-Model. *Journal of Irrigation and Drainage Engineering.* 133(4), 380-394.

Arellano, I. H., Madani, S. H., Huang, J. & Pendleton, P. (2016). Carbon dioxide adsorption by zinc-functionalized ionic liquid impregnated into bio-templated mesoporous silica beads. *Chemical Engineering Journal*, 283, 692-702.

Arellano, M. & Irmak, S. (2016). Reference (potential) evapotranspiration. I: Comparison of temperature, radiation, and combination-based energy balance equations in humid, subhumid, arid, semiarid, and Mediterranean-type climates. *Journal of Irrigation and Drainage Engineering*, 142(4), 04015065.

Arora, K. R. (2002). Irrigation water power and water resources engineering, Standard Publishers Distributors, New Delhi. 4th edition, Reprinted in 2009.

Audu, M. O., Isikwue, B. C. & Eweh, E. J. (2015). Evaluation of seasonal and annual variations of evapotranspiration with climatic parameters in Ibadan, Nigeria. *Journal of Earth Sciences and Geotechnical Engineering*, 5(2), 69-79.

Bai, J., Chen, X., Dobermann, A., Yang, H., Cassman, K. G. & Zhang, F. (2010). Evaluation of NASA satellite-and model-derived weather data for simulation of maize yield potential in China. *Agronomy Journal*, 102(1), 9-16.

Barella-Ortiz, A., Polcher, J., Tuzet, A. & Laval, K. (2013). Potential evaporation estimation through an unstressed surface-energy balance and its sensitivity to climate change. *Hydrology and Earth System Sciences*, 17(11), 4625-4639.

Behera, S. K. & Bahidar, C. (2020). Methods for evapotranspiration in hydrological models. *International Journal of Modern Agriculture*, 9(3), 469-474.

Biggs, T. W., Marshall, M. & Messina, A. (2016). Mapping daily and seasonal evapotranspiration from irrigated crops using global climate grids and satellite imagery: Automation and methods comparison. *Water Resources Research*, 52(9), 7311-7326.

Chandler, W. S., Whitlock, C. H. & Stackhouse, P. W. (2004). NASA Climatological Data for Renewable Energy Assessment. *Journal of Solar Energy Engineering*, 126, 945–949, https://doi.org/10.1115/1.1748466.

Costa, M. H., Biajoli, M. C., Sanches, L., Malhado, A. C., Hutyra, L. R., Da Rocha, H. R., ... & de Araújo, A. C. (2010). Atmospheric versus vegetation controls of Amazonian tropical rain forest evapotranspiration: Are the wet and seasonally dry rain forests any different? *Journal of Geophysical Research: Biogeosciences*, 115(G4).

Darshana, P., Shrivastava, P. K. & Patel, D. P. (2013). Study on noise pollution in Navsari city of South Gujarat, India. *Journal of Environmental Research and Development*, 8(2), 291-298.

de Noblet-Ducoudré, N. & Pitman, A. J. (2021). Terrestrial Processes and Their Roles in Climate Change. In *Oxford Research Encyclopedia of Climate Science*.

DehghaniSanij, H., Yamamoto, T. & Rasiah, V. (2004). Assessment of evapotranspiration estimation models for use in semi-arid environments. *Agricultural water management*, 64(2), 91-106.

Didari, S. & Ahmadi, S. H. (2019). Calibration and evaluation of the FAO56-Penman-Monteith, FAO24-radiation, and Priestly-Taylor reference evapotranspiration models using the spatially measured solar radiation across a large arid and semi-arid area in southern Iran. *Theoretical and Applied Climatology*, 136(1), 441-455.

Doorenbos, J. & Kassam, A. H. (1979). Yield response to water. *Irrigation and drainage paper*, 33, 257.

Dorrenbus, J. & Pruitt, W. O. (1977). Guidelines for predicting crop water requirements, FAO Irrigation and Drainage pap. No. 1, Rome, 34 pp.

Du, C., Yu, J., Wang, P. & Zhang, Y. (2016). Reference evapotranspiration changes: Sensitivities to and contributions of meteorological factors in the Heihe River Basin of Northwestern China (1961–2014). *Advances in Meteorology*, *2016*.

Duru, (2016). Optimization of Blaney-Morin-Nigeria (BMN) model for estimating evapotranspiration in Enugu, Nigeria. *African Journal of Agricultural Research*, 11(20), 1842-1848.

Ewemoje, T. A. & Umego, M. O. (2018). Trend analysis of reference evapotranspiration; case study of Asaba and Uyo, South-south Nigeria. In *2018 ASABE Annual International Meeting* (p.1). American Society of Agricultural and Biological Engineers.

Food and Agriculture Organization of the United Nations (FAO) (2015). Statistical Database. Available at http://www. faostat.org.

Food and Agriculture Organization of the United Nations (FAO) (2007). The Relationship between Water, Agriculture, Food Security and Poverty. FAO, Rome, Italy

Gao, X., Zhang, D., Chen, Z., Pal, J. S. & Giorgi, F. (2007). Land use effects on climate in China as simulated by a regional climate model. *Science in China Series D: Earth Sciences*, 50(4), 620-628.

Garg, T., Kumar, N., Chauhan, T. & Kango, R. (2016). Estimation of Reference Evapotranspiration using the FAO Penman-Monteith Method for Climatic Conditions of Himachal Pradesh India. In *Proceedings of National Conference: Civil Engineering Conference–Innovation for Sustainability (CEC–2016)* (Vol. 9, p. 10th).

Gedamu, A. (2017). *Remote Sensing-Based Estimation Of Evapotranspiration For Irrigation Performance Assessment* (Doctoral dissertation).

Gotardo, J. T., Rodrigues, L. N. & Gomes, B. M. (2016). Comparison of methods for estimating reference evapotranspiration: An approach to the management of water resources within an experimental basin in the Brazilian cerrado. *Engenharia Agrícola*, 36, 1016-1026.

Grattan, S. R. & Grieve, C. M. (1998). Salinity–mineral nutrient relations in horticultural crops. *Scientia horticulturae*, 78(1-4), 127-157.

Hargreaves, G. H. & Samani, Z. A. (1982). Estimating potential evapotranspiration. *Journal of the Irrigation and Drainage Division*, 108(3), 225-230.

Hargreaves, G. H. & Samani, Z. A. (1985). Reference crop evapotranspiration from temperature. *Applied Engineering in Agriculture*, 1(2), 96-99.

Hargreaves, G. H. (1994). Defining and using reference evapotranspiration. *Journal of Irrigation and Drainage Engineering*, 120(6), 1132-1139.

Hickman, J. M. (2011). Evaluating the Role of Evapotranspiration in the Hydrology of Bioinfiltration and Bioretention Basins Using Weighing Lysimeters. A Thesis in Civil Engineering Submitted in partial fulfillment of the requirements for the degree of Master of Science. The Graduate School of Novanova University.

Hosseinzadeh, F., Kowal, J. & Bouchard, P. J. (2014). Towards good practice guidelines for the contour method of residual stress measurement. *The Journal of Engineering*, 2014(8), 453-468.

Huizhi, L. & Jianwu, F. (2012). Seasonal and inter annual variations of evapotranspiration and energy exchange over different land surfaces in a semiarid area of China. *Journal of Applied Meteorology and Climatology*, 51(10), 1875-1888.

Irmak, S., Kabenge, I., Skaggs, K. E. & Mutiibwa, D. (2012). Trend and magnitude of changes in climate variables and reference evapotranspiration over 116-yr period in the Platte River Basin, central Nebraska–USA. *Journal of Hydrology*, 420, 228-244.

Itenfisu, D., Elliott, R. L., Allen, R. G. & Walter, I. A. (2003). Comparison of reference evapotranspiration calculations as part of the ASCE standardization effort. *Journal of Irrigation and Drainage Engineering*, 129(6), 440-448.

Jia, L., Zheng, C., Hu, G. & Menenti, M. (2018). Evapotranspiration. *Comprehensive Remote Sensing; Liang, S., Ed.; Elsevier: Amsterdam, The Netherlands*, 25-50.

Kang, S., Hu, X., Jerie, P. & Zhang, J. (2003). The effects of partial rootzone drying on root, trunk sap flow and water balance in an irrigated pear (Pyrus communis L.) orchard. *Journal of Hydrology*, 280(1-4), 192-206.

Kaspyap. P. S. & Panda, R. K. (2001). Evaluation of Evapotranspiration methods and development of crop coefficients for potato crop in a sub-humid region. Agricultural Water Management, 50, 9-25.

Kosa, P. (2003). The effect of temperature on actual evapotranspiration based on landsat 5 TM satellite imagery, (www.interchopen.com/download/pdf/ pafsid/14187).

Kosa, P. (2011). The effect of temperature on actual evapotranspiration based on Landsat 5 TM Satellite Imagery. *Evapotranspiration*, 56(56), 209-228.

Kousari, M. R., Ahani, H. & Hendi-zadeh, R. (2013). Temporal and spatial trend detection of maximum air temperature in Iran during 1960–2005. *Global and planetary change*, 111, 97-110.

Kuti, A., Adabembe, B. A., Musa, J. J., Adeoye, P. A., Animashaun, M. I., Aroboinsen, H. & Akhare, M. E. (2018). Assessment of Soil Salinity and Irrigation Water Quality of Chanchaga Irrigation Scheme I, Minna, Niger State. *FUOYE Journal of Engineering and Technology*, 3(1), 57-60.

Kuti, I. A., Murtala, A. I., Babatunde, O. & Suleiman, A. (2015). Trend analysis of hydro-meteorological data for river Kaduna at Shiroro Dam Site, Niger State Nigeria. *Journal of Scientific Research and Reports*, 1-12.

Kuti, I. A., Musa, J. J., Ibraheem I., Abdullahi, S., Adabembe, B. A. & Aroboinosen, H. (2016). Estimating Crop Evapotranspiration Rates for Spinach in Minna, Niger State. Proceedings of the 7th International Conference of Nigeria Association of Hydrological Sciences (NAHS), 7, 82- 89

Linsley, R. K., Kohler, M. A. & Paulhus, J. L. H. (1982). Hydrology for engineers. McGraw-Hill International Book Company. 3rd Edition.

Ma, L., Ahuja, L. R., Islam, A., Trout, T. J., Saseendran, S. A. & Malone, R. W. (2017). Modeling yield and biomass responses of maize cultivars to climate change under full and deficit irrigation. *Agricultural Water Management*, 180, 88-98.

Mansour, M., Hachicha, M. & Mougou, A. (2017). Trend analysis of potential evapotranspiration case of Chott-Meriem region (the Sahel of Tunisia). *International Journal of Agriculture Innovations and Research*, *5*(5), 703-708.

Moorhead, E. J. (2018). Field-Scale Estimation of Evapotranspiration: Advanced Evapotranspiration Methods and Applications. USDA-ARS Conservation and Production Research Laboratory, Bushland, TX, USA.

Nathan, E. D., Raymond, E. K. & Bruce, R. M. (2002). Construction and Performance of Large Soil Core Lysimeters. Department of Soil Science, North Dakota State University, Fargo, ND53 105-5638.

Nova, N. V., Pereira, A. B. & Shock, C. C. (2007). Estimation of reference evapotranspiration by an energy balance approach. *Biosystems Engineering*, 96(4), 605-615.

Ohmura, A. & Wild, M. (2002). Is the hydrological cycle accelerating. *Science*, 298(5597), 1345-1346.

Ohunakin, O. S., Adaramola, M. S., Oyewola, O. M., Matthew, O. J. & Fagbenle, R. O. (2015). The effect of climate change on solar radiation in Nigeria. *Solar Energy*, 116, 272-286.

Pereira, L. S., Allen, R. G., Smith, M. & Raes, D. (2015). Crop evapotranspiration estimation with FAO56: Past and future. *Agricultural Water Management*, 147, 4-20.

Richard, H. W. & Steven, W. R. (2007). CHAPTER 2 - Water Cycle. Forest Ecosystems (Third Edition), Academic Press, Elsevier. Pp 19-57, ISBN 9780123706058. https://doi.org/10.1016/B978-012370605-8.50007-4.

Rim, C. S. (2009). Spatial Distribution of Precipitation Trends According to Geographical and Topographical Conditions. *Journal of Korea Water Resources Association*, 42(5), 385-396.

Sabziparvar, A. A. & Tabari, H. (2010). Regional estimation of reference evapotranspiration in arid and semiarid regions. *Journal of Irrigation and Drainage Engineering*, 136(10), 724-731.

Senatore, A., Davolio, S., Furnari, L. & Mendicino, G. (2020). Reconstructing flood events in Mediterranean coastal areas using different reanalyses and high-resolution meteorological models. *Journal of Hydrometeorology*, 21(8), 1865-1887.

Shirish, S. (1996). Changes in the photosynthetic rate, transpiration rate, stomatal conductivity and water use efficiency of vitis varieties grown under different temperature and light conditions. Science Bulletin of the Faculty of Agriculture, Kyushu University. 51(1–2), 33–38

Shuyun, F., Liu, J., Zhang, Q., Zhang, Y., Singh, V. P., Gu, X. & Sun, P. (2020). A global quantitation of factors affecting evapotranspiration variability. *Journal of Hydrology*, 584, 124688.

Tabari, H. (2010). Evaluation of reference crop evapotranspiration equations in various climates. *Water resources management*, 24(10), 2311-2337.

Tabari, H., Grismer, M. E. & Trajkovic, S. (2013). Comparative analysis of 31 reference evapotranspiration methods under humid conditions. *Irrigation Science*, 31(2), 107-117.

Tabari, H., Somee, B. S. & Zadeh, M. R. (2011). Testing for long-term trends in climatic variables in Iran. *Atmospheric research*, 100(1), 132-140.

Tyagi, N. K., Sharma, D. K. & Luthra, S. K. (2000). Determination of Evapotranspiration and crop coefficient of rice and sunflower with lysimeter. Elsevier. *Agricultural Water Management*, 45(2000), 41-54.

Wang, X., Yang, G., Feng, Y., Ren, G. & Han, X. (2012). Optimizing feeding composition and carbon–nitrogen ratios for improved methane yield during anaerobic co-digestion of dairy, chicken manure and wheat straw. *Bioresource technology*, 120, 78-83.

Xu, C. Y., Gong, L., Jiang, T., Chen, D. & Singh, V. P. (2006). Analysis of spatial distribution and temporal trend of reference evapotranspiration and pan evaporation in Changjiang (Yangtze River), catchment. *Journal of hydrology*, 327(1-2), 81-93.

Yang, X., Gao, W., Shi, Q., Chen, F. & Chu, Q. (2013). Impact of climate change on the water requirement of summer maize in the Huang-Huai-Hai farming region. *Agricultural Water Management*, 124, 20-27.

Yoder, R. E., Odhiambo, L. O. & Wright, W. C. (2005). Evaluation of methods for estimating daily reference crop evapotranspiration at a site in the humid southeast United States. *Applied Engineering in Agriculture*, 21(2), 197-202.

Zotarelli, L., Dukes, M. D., Romero, C. C., Migliaccio, K. W. & Morgan, K. T. (2010). Step by step calculation of the Penman-Monteith Evapotranspiration (FAO-56 Method). *Institute of Food and Agricultural Sciences. University of Florida*.

APPENDICES

Appendix I: Minna Reference Evapotranspiration

Year	Jan	Feb	Mar	Apr	May	Jun	Jul	Aug	Sep	Oct	Nov	Dec
1982	3.26	3.40	3.13	2.39	1.99	1.74	1.73	1.58	1.72	1.84	2.84	3.04
1983	4.04	3.45	3.93	3.17	2.26	1.75	1.69	1.55	1.73	2.57	2.88	2.81
1984	3.54	3.36	2.77	2.52	2.11	2.04	1.88	1.83	1.87	2.15	2.75	3.21
1985	3.11	4.33	3.02	2.73	2.26	1.94	1.82	1.70	1.78	2.36	2.79	3.35
1986	3.61	2.84	2.79	2.77	2.25	2.11	1.69	1.84	1.89	2.24	2.80	3.44
1987	3.70	3.42	3.35	3.46	3.02	1.98	1.81	1.70	1.91	2.31	3.18	3.39
1988	3.61	3.81	3.17	2.87	2.32	1.83	1.71	1.53	1.83	2.50	3.03	2.99
1989	4.12	4.48	2.95	2.96	2.38	1.89	1.77	1.63	1.82	2.22	3.02	3.02
1990	3.26	4.02	4.30	2.77	2.17	1.99	1.76	1.75	1.81	2.21	2.74	2.89
1991	3.77	3.09	3.25	2.74	2.02	1.95	1.67	1.54	1.88	1.96	3.01	3.35
1992	4.17	5.07	3.71	2.99	2.30	1.83	1.62	1.58	1.74	2.14	2.97	3.29
1993	4.00	4.00	3.39	3.13	2.32	1.88	1.68	1.70	1.84	2.17	2.60	3.14
1994	3.37	3.96	2.91	2.64	2.16	1.90	1.66	1.40	1.67	1.99	2.82	3.22
1995	3.39	3.70	2.93	2.62	2.30	1.98	1.74	1.61	1.86	2.04	2.80	2.96
1996	3.21	3.17	2.82	2.67	2.29	1.88	1.75	1.61	1.73	2.17	3.11	3.16
1997	3.29	4.40	3.16	2.57	2.16	1.90	1.79	1.79	1.97	2.00	2.78	3.17
1998	3.71	4.08	4.20	2.73	2.23	2.00	1.67	1.67	1.90	2.16	3.11	3.25
1999	3.45	3.25	2.99	3.10	2.64	2.23	2.00	1.85	2.00	2.55	4.35	5.63
2000	6.07	7.49	6.09	4.00	3.03	1.81	1.68	1.77	1.84	2.30	3.21	3.42
2001	4.74	5.13	3.91	2.94	2.35	1.90	1.84	1.55	1.87	2.71	4.10	4.84
2002	6.19	5.46	3.90	2.86	2.43	2.01	1.81	1.79	1.91	2.25	3.47	4.47
2003	4.67	4.37	4.39	2.92	2.75	2.15	1.94	1.75	1.96	2.20	3.21	4.29
2004	4.55	5.64	5.42	3.42	1.98	1.83	1.86	1.81	1.90	2.30	3.50	4.62
2005	6.10	4.81	4.01	3.84	3.12	2.30	2.02	2.21	2.01	2.33	3.73	4.82
2006	4.78	4.74	4.50	4.31	2.67	2.38	2.07	1.69	1.85	2.30	3.94	4.89
2007	6.07	5.32	4.97	3.73	2.64	1.93	1.73	1.62	1.89	2.25	2.95	3.58
2008	4.12	4.69	3.31	3.21	2.70	2.04	1.78	1.75	1.97	2.43	3.35	3.38
2009	3.35	3.45	3.78	2.58	2.34	1.88	1.86	1.74	1.97	1.91	2.99	3.54
2010	3.60	3.52	3.91	2.99	2.17	1.95	1.68	1.68	1.81	1.94	2.82	3.56
2011	3.91	3.02	3.32	3.06	2.13	1.91	1.80	1.65	1.91	2.17	3.36	3.75
2012	3.75	3.30	4.27	2.93	2.14	1.95	1.71	1.69	1.86	2.14	2.90	3.38
2013	3.36	3.23	2.85	2.77	2.23	1.89	1.88	1.74	1.93	2.48	3.33	4.24
2014	4.41	5.21	3.90	3.11	2.40	2.04	1.96	1.69	1.81	2.19	3.29	4.91
2015	5.52	4.49	4.67	4.75	3.55	2.32	1.97	1.58	1.94	2.15	4.39	5.82
2016	6.56	6.46	4.12	3.43	2.85	2.10	1.80	1.76	1.90	2.41	3.64	4.47
2017	4.50	6.00	5.11	4.36	2.59	2.12	1.92	1.73	1.97	2.69	3.91	4.25
2018	5.27	4.23	4.01	3.79	2.69	1.99	1.83	1.71	1.90	2.25	3.54	4.21

Year	Jan	Feb	Mar	Apr	May	Jun	Jul	Aug	Sep	Oct	Nov	Dec
2019	4.45	4.69	3.98	4.03	2.69	2.08	1.99	1.81	1.82	1.90	3.03	4.04
2020	4.65	5.21	3.77	3.30	2.72	2.09	1.83	1.91	1.86	2.65	3.67	3.95

Appendix II: Shiroro Reference Evapotranspiration

Year	Jan	Feb	Mar	Apr	May	Jun	Jul	Aug	Sep	Oct	Nov	Dec
1982	3.89	4.27	3.83	2.53	1.98	1.66	1.71	1.53	1.71	1.89	3.30	3.75
1983	5.32	4.55	5.51	3.84	2.38	1.73	1.55	1.51	1.80	2.91	3.43	3.40
1984	4.45	4.22	3.17	2.73	2.08	1.96	1.85	1.83	1.88	2.24	3.19	3.90
1985	3.76	5.77	3.61	3.12	2.27	1.84	1.76	1.66	1.82	2.60	3.27	4.17
1986	4.59	3.57	3.20	2.96	2.37	2.05	1.63	1.85	1.89	2.44	3.15	4.20
1987	4.67	4.43	4.05	4.62	3.39	1.97	1.79	1.68	1.91	2.46	3.70	4.20
1988	4.58	5.04	4.14	3.13	2.38	1.77	1.59	1.41	1.78	2.76	3.57	3.64
1989	5.43	6.18	3.85	3.41	2.45	1.85	1.73	1.56	1.76	2.39	3.56	3.74
1990	4.13	5.42	6.27	3.08	2.13	1.89	1.70	1.76	1.85	2.33	3.07	3.24
1991	4.81	3.49	3.89	2.94	1.93	1.90	1.60	1.43	1.86	2.03	3.50	4.12
1992	4.70	6.37	4.15	3.05	2.19	1.74	1.59	1.49	1.79	2.21	3.37	3.84
1993	4.72	4.88	4.00	3.50	2.30	1.84	1.64	1.64	1.86	2.26	2.95	3.75
1994	4.02	5.07	3.28	2.89	2.19	1.81	1.55	1.36	1.63	2.07	3.36	4.06
1995	4.28	4.65	3.58	2.93	2.30	1.91	1.71	1.56	1.85	2.12	3.31	3.64
1996	3.94	3.97	3.28	3.01	2.27	1.82	1.67	1.59	1.71	2.30	3.66	3.90
1997	4.13	6.12	4.08	2.78	2.19	1.89	1.70	1.76	2.03	2.10	3.17	3.89
1998	4.70	5.53	5.88	3.05	2.18	1.94	1.57	1.58	1.90	2.29	3.59	3.97
1999	4.27	4.02	3.61	3.78	2.91	2.30	1.77	1.65	1.91	2.62	5.26	7.19
2000	7.72	9.22	7.77	4.44	3.28	1.82	1.63	1.76	1.83	2.39	3.65	4.00
2001	4.93	5.56	4.35	3.08	2.41	1.86	1.75	1.48	1.89	2.99	4.11	5.36
2002	7.28	6.84	4.67	3.11	2.52	1.92	1.76	1.79	1.94	2.44	3.69	4.69
2003	5.17	5.24	5.51	3.11	2.91	2.03	1.89	1.67	2.00	2.36	3.60	4.88
2004	5.48	7.47	6.88	3.51	2.02	1.85	1.96	1.78	2.03	2.61	4.62	6.35
2005	7.58	6.16	4.90	4.13	3.37	2.27	2.03	2.03	2.10	2.65	5.02	6.19
2006	5.98	5.37	5.38	5.23	2.78	2.46	2.05	1.72	1.87	2.53	4.91	6.29
2007	7.81	6.87	6.48	3.75	2.74	1.89	1.70	1.64	1.99	2.40	3.39	4.22
2008	4.89	6.64	4.00	3.86	3.01	2.13	1.78	1.70	2.01	2.69	3.90	4.18
2009	4.22	4.71	5.19	2.97	2.51	1.95	1.83	1.75	2.01	1.99	3.72	4.80
2010	4.99	4.88	5.69	3.73	2.32	1.99	1.63	1.63	1.82	2.01	3.25	4.60
2011	5.80	4.11	5.00	4.22	2.38	1.95	1.87	1.65	2.01	2.40	4.19	5.28
2012	5.40	4.96	6.68	3.42	2.26	1.94	1.68	1.67	1.86	2.23	3.38	4.16
2013	4.16	4.14	3.25	3.21	2.36	1.95	1.90	1.69	1.97	2.86	4.51	5.92
2014	6.37	7.41	4.64	3.44	2.60	2.07	1.92	1.65	1.81	2.38	3.73	5.62
2015	6.75	5.80	5.62	6.16	3.35	1.99	1.85	1.58	1.98	2.18	4.02	5.26
2016	6.66	7.21	3.97	3.31	2.50	2.06	1.74	1.72	1.95	2.56	3.69	4.45
2017	4.57	6.91	5.64	4.24	2.44	2.12	1.87	1.64	1.95	2.90	3.91	4.29
2018	5.77	4.50	4.07	3.54	2.36	1.87	1.81	1.66	2.00	2.30	3.76	4.57
2019	4.92	5.32	4.43	3.99	2.50	2.06	1.84	1.74	1.89	1.96	3.26	4.39
2020	5.15	6.19	4.03	2.91	2.44	2.01	1.67	1.75	1.86	2.74	3.64	4.04

Appendix III: Bida Reference Evapotranspiration between 1982 and 2020

Year	Jan	Feb	Mar	Apr	May	Jun	Jul	Aug	Sep	Oct	Nov	Dec
1982	3.09	3.17	2.98	2.62	2.14	1.90	1.89	1.74	1.86	2.05	2.75	2.82
1983	3.40	3.22	3.59	3.32	2.42	1.89	1.89	1.70	1.81	2.54	2.74	2.63
1984	3.24	3.14	2.85	2.74	2.30	2.23	2.00	2.00	1.96	2.24	2.69	3.04
1985	2.92	3.83	3.07	2.89	2.57	2.16	1.90	1.79	1.89	2.39	2.73	3.14
1986	3.37	2.97	2.98	3.06	2.40	2.33	1.83	1.92	1.97	2.30	2.78	3.23
1987	3.51	3.35	3.45	3.43	3.35	2.16	1.96	1.82	2.06	2.37	3.04	3.25
1988	3.36	3.52	3.19	3.10	2.56	2.02	1.85	1.74	1.95	2.47	2.92	2.83
1989	3.60	3.91	3.01	3.15	2.54	2.05	1.88	1.77	1.96	2.28	2.90	2.92
1990	3.02	3.57	3.82	3.11	2.36	2.23	1.86	1.90	1.95	2.34	2.76	2.94
1991	3.59	3.37	3.42	3.06	2.23	2.14	1.81	1.75	1.98	2.13	2.92	3.24
1992	4.01	4.73	4.02	3.27	2.54	2.02	1.78	1.78	1.78	2.28	2.94	3.16
1993	3.70	3.91	3.59	3.40	2.67	2.04	1.79	1.84	1.91	2.34	2.66	3.07
1994	3.28	3.73	3.21	2.92	2.37	2.09	1.77	1.57	1.78	2.07	2.78	3.04
1995	3.28	3.73	3.21	2.92	2.37	2.09	1.77	1.57	1.78	2.07	2.78	3.04
1996	3.12	3.37	2.99	2.81	2.46	2.11	1.86	1.70	1.97	2.14	2.74	2.79
1997	2.94	2.93	2.90	2.78	2.51	2.03	1.89	1.71	1.87	2.22	2.97	2.93
1998	3.33	3.69	3.92	2.88	2.44	2.13	1.82	1.81	1.95	2.31	3.04	3.08
1999	3.23	3.22	3.38	3.42	3.03	2.56	2.36	2.15	2.28	2.82	4.01	4.55
2000	4.93	6.03	5.29	4.08	3.24	1.91	1.79	1.84	1.98	2.34	3.08	3.17
2001	4.32	4.66	3.99	3.16	2.58	2.13	2.07	1.82	2.07	2.69	3.91	4.52
2002	5.31	4.68	3.90	3.11	2.68	2.33	2.02	1.85	2.10	2.33	3.41	4.31
2003	4.26	4.18	4.08	3.04	2.93	2.35	2.12	1.93	2.04	2.30	3.11	3.99
2004	4.08	4.89	5.02	3.62	2.17	2.04	1.96	1.98	2.09	2.45	3.34	3.90

2005	5.07	4.31	3.99	3.98	3.18	2.48	2.21	2.54	2.05	2.40	3.50	4.22
2006	4.34	4.45	4.36	4.18	2.86	2.55	2.22	1.79	1.94	2.36	3.68	4.12
2007	4.76	4.59	4.47	3.90	2.86	2.18	1.92	1.68	1.93	2.34	2.84	3.28
2008	3.72	3.98	3.35	3.35	2.83	2.22	1.91	1.82	2.01	2.44	3.13	3.18
2009	3.13	3.21	3.55	2.73	2.45	2.01	1.97	1.80	2.05	2.06	2.95	3.22
2010	3.23	3.41	3.58	3.14	2.34	2.12	1.80	1.80	1.89	2.04	2.78	3.26
2011	3.27	2.88	3.10	2.92	2.26	2.00	1.90	1.78	1.95	2.32	3.09	3.26
2012	3.21	3.07	3.62	3.10	2.35	2.13	1.79	1.71	1.89	2.25	2.79	3.15
2013	3.07	3.02	3.14	2.97	2.46	2.07	1.95	1.93	2.03	2.55	3.24	3.81
2014	3.68	4.36	3.82	3.28	2.58	2.31	2.22	1.86	1.94	2.31	3.19	4.30
2015	4.65	4.21	4.29	4.41	3.79	2.59	2.13	1.71	1.99	2.33	4.08	5.29
2016	5.53	5.21	4.31	3.71	3.03	2.27	1.91	1.93	2.04	2.45	3.68	4.33
2017	4.18	5.23	4.74	4.45	2.74	2.26	2.09	1.92	2.04	2.66	3.65	4.03
2018	4.58	3.96	4.31	4.12	2.92	2.16	1.96	1.85	1.95	2.35	3.38	3.93
2019	4.19	4.36	4.20	4.44	3.00	2.28	2.21	1.93	1.91	1.99	2.93	3.66
2020	4.17	4.53	3.83	3.69	2.99	2.26	1.98	2.21	1.84	2.59	3.62	3.77